Cellular & Molecular Immunology (2016) 13, 747–763

www.nature.com/cmi

RESEARCH ARTICLE

The IRAK-ERK-p67phox-Nox-2 axis mediates TLR4, 2-induced ROS production for IL-1β transcription and processing in monocytes

Ankita Singh[1], Vishal Singh[1], Rajiv L. Tiwari[1], Tulika Chandra[2], Ashutosh Kumar[3], Madhu Dikshit[1] and Manoj K. Barthwal[1]

In monocytic cells, Toll-like receptor 4 (TLR4)- and TLR2-induced reactive oxygen species (ROS) cause oxidative stress and inflammatory response; however, the mechanism is not well understood. The present study investigated the role of interleukin-1 receptor-associated kinase (IRAK), extracellular signal-regulated kinase (ERK), p67phox and Nox-2 in TLR4- and TLR2-induced ROS generation during interleukin-1 beta (IL-1β) transcription, processing, and secretion. An IRAK1/4 inhibitor, U0126, PD98059, an NADPH oxidase inhibitor (diphenyleneiodonium (DPI)), and a free radical scavenger (N-acetyl cysteine (NAC))-attenuated TLR4 (lipopolysaccharide (LPS))- and TLR2 (Pam3csk4)-induced ROS generation and IL-1β production in THP-1 and primary human monocytes. An IRAK1/4 inhibitor and siRNA-attenuated LPS- and Pam3csk4-induced ERK-IRAK1 association and ERK phosphorylation and activity. LPS and Pam3csk4 also induced IRAK1/4-, ERK- and ROS-dependent activation of activator protein-1 (AP-1), IL-1β transcription, and IL-1β processing because significant inhibition in AP-1 activity, IL-1β transcription, Pro- and mature IL-β expression, and caspase-1 activity was observed with PD98059, U0126, DPI, NAC, an IRAK1/4 inhibitor, tanshinone IIa, and IRAK1 siRNA treatment. IRAK-dependent ERK-p67phox interaction, p67phox translocation, and p67phox–Nox-2 interaction were observed. Nox-2 siRNA significantly reduced secreted IL-1β, IL-1β transcript, pro- and mature IL-1β expression, and caspase-1 activity indicating a role for Nox-2 in LPS- and Pam3csk4-induced IL-1β production, transcription, and processing. In the present study, we demonstrate that the TLR4- and TLR2-induced IRAK-ERK pathway cross-talks with p67phox-Nox-2 for ROS generation, thus regulating IL-1β transcription and processing in monocytic cells.
Cellular & Molecular Immunology (2016) **13**, 747–763;doi:10.1038/cmi.2015.62;published online 31 August 2015

Keywords: IL-1β; IRAK; monocytes; ROS; TLR

INTRODUCTION

Toll-like receptor (TLR)-induced reactive oxygen species (ROS) can exert deleterious effects by inducing oxidative stress and cytokine overproduction[1] leading to sepsis, septic shock, rheumatoid arthritis, and diabetic complications. In case of sterile infections, where danger-associated molecular patterns (DAMPs) activate TLRs, the released ROS may be detrimental to host tissues.[2] TLR2 and TLR4 can regulate bacterial sepsis and shock by inducing interleukin-1 beta (IL-1β) production.[3]

IL-1β-driven inflammation is involved in the progression of many inflammatory disorders.[4] The secretory signal sequence is absent in IL-1β, and its secretion is divided into steps.[5] First, TLR activation leads to the transcription and accumulation of the precursor protein pro-IL-1β. The second step involves the processing of pro-IL-1β into mature IL-1β by the inflammasome, which activates caspase-1, a proteolytic enzyme responsible for the cleavage and secretion of cytokines.[6] Due to a gain-of-function mutation in NLRP3, such as in familial cold autoinflammatory syndrome, Muckle–Wells syndrome, and

[1]Pharmacology Division, CSIR-Central Drug Research Institute, B.S. 10/1, Sector 10, Sitapur Road, Jankipuram Extension, Lucknow 226031, Uttar Pradesh, India; [2]Department of Transfusion Medicine and Blood Bank, King George's Medical University, Lucknow, Uttar Pradesh, India and [3]Department of Pathology, King George's Medical University, Lucknow, Uttar Pradesh, India
Correspondence: Dr. MK Barthwal, Pharmacology Division, CSIR-Central Drug Research Institute, B.S 10/1, Sector 10, Jankipuram Extension, Sitapur Road, Lucknow-226031, Uttar Pradesh, India.
E-mail: manojbarthwal@cdri.res.in
Received: 11 December 2014; Revised: 1 June 2015; Accepted: 3 June 2015

neonatal onset multisystem inflammatory disease (NOMID), autoinflammatory disorders can be treated with an IL-1 receptor antagonist (IL-1Ra) or monoclonal anti-IL-1β antibodies (Abs).[7] Various extracellular signals involved in inflammasome assembly have been identified; however, the molecular mechanisms involved in caspase-1 activation and IL-1β processing and secretion are still only partially understood.[8]

The signaling of two receptor families, TLRs and IL-1Rs, is mediated through a unique family of protein kinases known as interleukin-1 receptor-associated kinases (IRAKs).[9] Pharmacologic inhibition of both IRAK4 and IRAK1 might be necessary to block pro-inflammatory cytokine production,[10,11] indicating the importance of IRAK signaling in inflammatory cytokine secretion. Previously, we suggested a novel mechanism of phorbol 12-myristate 13-acetate (PMA)-induced IL-1β production involving protein kinase C-δ (PKC-δ) in monocytes.[12] TLR engagement by various ligands also activates the mitogen-activated protein kinase (MAPK) cascade.[13] The MAPK family members p38 MAPK, c-Jun amino-terminal kinase (JNK), and extracellular signal-regulated kinase (ERK), which are downstream of TLR, are involved in innate immunity and can induce the production of cytokines and inflammatory mediators.[14]

Recently, the role of ROS in IL-1β secretion has attracted intense interest.[15] The multi-component enzyme complex NADPH oxidase (Nox) is a potential source of ROS. The translocation of cytosolic components (p47phox and p67phox) to the membrane is a prerequisite for NADPH oxidase activation.[16] It has been reported that pattern recognition receptor (PRR) engagement activates NADPH oxidase through the generation of ROS and caspase-1 induction, leading to secretion of mature IL-1β.[17] Nox-2 is the predominant NADPH oxidase in macrophages,[18] and TLRs can regulate Nox isozymes.[19] However, the predominant Nox isoforms involved in ROS generation after specific TLR activation during IL-1β secretion remain unclear.

The present study demonstrates the role of the IRAK-ERK-p67phox-Nox-2 axis in TLR2, 4-induced ROS, which in turn regulate IL-1β transcription, processing, and secretion.

MATERIALS AND METHODS

Pharmacological inhibitors, including an IRAK1/4 inhibitor, U0126, PD98059, and Pam3csk4, were purchased from Calbiochem (San Diego, CA, USA). Lipopolysaccharide (LPS), a protease inhibitor mixture, and Abs against β-actin and p-p47phox were obtained from Sigma-Aldrich (St. Louis, MO, USA). The p44/42 MAP Kinase Assay kit (nonradioactive), p67phox, ERK1/2, p-ERK1/2 Abs, and ATP were procured from Cell Signaling Technology (Danvers, MA, USA). Anti-p-JNK and anti-total JNK were from Millipore (Billerica, MA, USA). Tanshinone IIa and Abs against human IRAK, Nox-2, TLR2, TLR4, p47phox, and IL-1β were purchased from Santa Cruz Biotechnology (Santa Cruz, CA, USA). Control small interfering RNA (siRNA), IRAK siRNAs, TLR2 siRNA, TLR4 siRNA, and Nox-2 siRNA were purchased from Santa Cruz Biotechnology (Santa Cruz, CA, USA) and Dharmacon (Chicago, IL, USA). The caspase-1 fluorometric assay kit was purchased from R&D Systems Inc. (Minneapolis, MN, USA). Light Cycler 480 SYBR Green I Master was obtained from Roche Applied Science (Mannheim, Germany), and the activator protein-1 (AP-1) activity ELISA kit (TransAMTM AP-1-c-Jun) was obtained from Active Motif Co. Ltd. (Carlsbad, CA, USA). ECL substrate was procured from GE Healthcare (Piscataway, NJ, USA), and reagents related to tissue culture were from Invitrogen (Carlsbad, CA, USA). Propidium iodide (PI), diphenyleneiodonium (DPI), N-acetyl cysteine (NAC), dichlorofluorescin (DCF), and all other chemicals used in the study were purchased from Sigma (St. Louis, MO, USA).

Isolation and culture of human monocytes

After obtaining informed consent from healthy donors, circulating human primary monocytes were isolated as previously described[20] with slight modifications. Permission for the study was obtained from the Institutional Ethics Committee (human research) of CSIR-Central Drug Research Institute (CSIR-CDRI) and King George's Medical University (KGMU), Lucknow. The ethical guidelines were in agreement with Helsinki Declaration. Buffy coats were subjected to dextran sedimentation followed by density gradient centrifugation utilizing Percoll 1080 and 1065 and hyperosmotic gradient. Then, monocytes were allowed to adhere for 1 h in RPMI-1640 media containing 10% fetal bovine serum (FBS) before use in experiments. Trypan blue staining was used to assess cell viability, and CD14 staining was evaluated by flow cytometry to assess sample purity. The viability and purity of the cells were both found to be more than 95%. THP1, a human monocytic cell line, was cultured in RPMI-1640 media with 100 IU mL^{-1} penicillin and 100 μg mL^{-1} streptomycin and was supplemented with 10% heat-inactivated FBS. Monocytic cells were treated for various time points with LPS or Pam3csk4 (100 ng mL^{-1})[12] and ATP (5 mmol L^{-1}).[21] A 1-h pre-treatment of pathway inhibitors was administered at the following concentrations: IRAK1/4 inhibitor (0.3 μmol L^{-1}); ERK1/2 pathway inhibitors (U0126 and PD98059; 10 μmol L^{-1}); NADPH oxidase inhibitor (DPI; 10 μmol L^{-1}); free radical scavenger (NAC; 10 mmol L^{-1}); JNK inhibitor II (10 μmol L^{-1}); AP-1 inhibitor (tanshinone IIa; 1 μmol L^{-1}); and vehicle dimethyl sulfoxide ($< 0.1\%$). The IRAK1/4 inhibitor used in the present study is a small-molecule inhibitor that selectively inhibits the kinase activities of IRAK1 and IRAK4 and has been previously used.[22] It has been shown to exhibit little activity against a panel of 27 other kinases (IC50 > 10 μM), including Lck and Src, suggesting the efficacy and specificity of the compound. IRAK phosphorylation was analyzed in the presence of the IRAK1/4 inhibitor to ensure its inhibition under the experimental conditions (Supplementary Figure S1). Similarly, AP-1 inhibition was observed with tanshinone IIa, indicating its efficacy (Supplementary Figure S2a). The cytotoxicity of DPI, NAC, tanshinone IIa, and IRAK1/4 inhibitor was analyzed by PI labeling. The level of cell death was not significantly altered, suggesting that the results

were due to inhibitor effects and not due to cytotoxicity (Supplementary Figure S2b). The concentration and duration of the inhibitors in the present study have shown minimal cytotoxicity under these experimental conditions.

IL-1β assay

Conventional ELISA (BD OptEIA set Human IL-1β, San Diego, CA, USA) was used to measure the production of IL-1β after treatment with LPS, Pam3csk4, and different pathway inhibitors in the media as described earlier.[12] In brief, the capture Ab was coated on the ELISA plates and incubated overnight at 4 °C. The collected supernatants from control and treated monocytic cells were incubated for 2 h at room temperature, washed, and incubated with the detection Ab. After washing, the enzyme reagent was incubated. Then, tetramethylbenzene (TMB) substrate was added to develop color, and the assay was subsequently read with an ELISA plate reader (Biotek Instrument, Winooski, VT, USA) at 450 nm and 570 nm. Standard IL-1β provided in the kit was used to calculate absolute IL-1β levels.[12]

Immunoblotting

After the desired treatments, cells were lysed in lysis buffer containing 0.1 M NaCl, 0.01 M Tris HCl (pH 7.4), 0.001 M EDTA (pH 7.4), aprotinin (1 μg mL^{-1}), phenylmethylsulfonyl fluoride (100 μg mL^{-1}), pepstatin (20 μg mL^{-1}), sodium orthovanadate (2 mM), sodium fluoride (2 mM) and 1% Triton X-100. Bicinchoninic acid (BCA) reagent was used to measure protein concentrations. Lysates containing equal amounts of protein were denatured at 100 °C for 5 min in Laemmli buffer and run on a denaturing 7–10% sodium dodecyl sulfate–polyacrylamide gel electrophoresis gel. Then, the proteins were transferred onto polyvinylidene fluoride (PVDF) membranes followed by blocking of the PVDF membranes with 5% bovine serum albumin in Tris-buffered saline and Tween 20. After blocking, the membrane was incubated with the following primary Abs as per the manufacturers' protocol: IRAK1 (1:1000); p-IRAK1 (1:1000); p-ERK1/2 (1:3000); ERK1/2 (1:3000); p67phox (1:3000); p-p47phox (1:3000); p47phox (1:1000); p-JNK (1:1000); JNK (1:1000); IL-1β (1:1000); Nox-2 (1:1000); and β-actin (1:2000). After primary Ab incubation, specific horseradish peroxidase (HRP)-conjugated secondary Abs were added. Enhanced chemiluminescence was used to detect the specific bands as previously described.[23] The protein bands were quantified by densitometry and normalized against their respective total protein expression, and β-actin was used as loading control. The quantification was performed on the basis of relative units using an ImageQuant, LAS 4000 biomolecular imager (GE Healthcare Bio-Science, Pittsburgh, PA, USA) and Quantity One software Bio-Rad, Hercules, CA, USA.

Immunoprecipitation and *in vitro* ERK kinase assay

Lysis buffer with 0.1% Nonidet P-40, 50 mM Tris-Cl (pH 8.0), 2 mM EDTA, 137 mM sodium chloride, 0.1% Nonidet P-40, and 5% glycerol was used to lyse the cells from different experimental groups. Pre-adsorption of Abs to protein-A Sepharose beads was performed in WG buffer (HEPES 1 M, NaCl 2 M, 10% Triton X-100) at 4 °C for 1 h. Then, the lysates were mixed with pre-adsorbed beads and incubated at 4 °C for 2 h. The protein A-Sepharose beads were washed, and the immunoprecipitates were processed for immunoblotting. ERK activity was assessed using the p44/42 MAP Kinase Assay kit. Briefly, the cell lysates were immunoprecipitated by an immobilized p44/42 Ab bead slurry and incubated overnight at 4 °C. Subsequently, the cell lysates were washed and re-suspended in 50 μL of 1X Kinase buffer supplemented with 200 μmol L^{-1} ATP, and 1 μL of ELK-1 was incubated for 30 min at 30 °C.[24] The reaction was then terminated by boiling in 3× SDS buffer. Phosphorylation of the ELK-1 protein was detected by western blotting using a Phospho-Elk-1 (Ser383) Ab.

AP-1 activity assay

A commercially available ELISA kit (TransAM AP-1-c-Jun; Active Motif, Carlsbad, CA, USA) was used for the preparation of nuclear extracts and AP-1 activity measurement. Microtiter plates used for AP-1 estimation were coated with oligonucleotides 5′-TGAGTCA-3′, and 10 μg of nuclear extract was loaded onto a well of a 96-well plate for 1 h. Then, the plates were washed three times and incubated with mAbs against c-Jun for an addition 1 h at RT. A total of 100 μL of anti-IgG-HRP conjugate was then added and incubated for 1 h at 25 °C. Then, TMB solution was added, and absorbance was measured at 450 nm. Absolute levels of AP-1 were quantified using standard curves.

Propidium iodide labeling

The cytotoxicity of various inhibitors was determined by PI labeling (excitation at 535 nm and emission at 615 nm), which only stains dead cells.[25] After the desired treatment, the cells were harvested and treated with PI (5 μg mL^{-1}) for 30 min, and cell viability was analyzed using the CellQuest program (FACSCalibur; Becton-Dickinson, Franklin Lakes, New Jersey, USA).[26]

siRNA transfection

An Amaxa nucleofector machine (Amaxa, Cologne, Germany) was used to perform transfections as previously described.[27] The optimized protocol for the transfection of THP1 (Cell Line Nucleofector kit V) and primary monocytes (Human Monocyte Nucleofector kit) provided by the manufacturer was used. Briefly, in 100 μL of transfection reagent, 1×10^6 cells were re-suspended and transfected with 100 nmol L^{-1} of control or IRAK1, IRAK4, Nox-2, TLR2, and TLR4 siRNA. The nucleofector machine program V001 was used for THP-1, and Y001 was used for primary monocytes. A total 1 mL of medium was pre-warmed in 6-well plates. After transfection, the cells were removed with 0.5 mL of RPMI-1640 and added to the pre-warmed plate. The respective treatments were administered 18 h after transfection. For monitoring the transfection efficiency, fluoroscein isothiocyanate-labeled control siRNA and expression of recombinant green fluorescent protein (provided in

the kit) was used. Gene silencing was measured by western blotting.

Caspase-1 fluorometric assay

Caspase-1 fluorometric assay kit (R&D Systems Inc., Minneapolis, MN, USA) was used to assess caspase-1 activity. After various treatments, the cells were lysed using cell lysis buffer provided with the kit. A total of 200 μg of total protein and an equal volume of 2× reaction buffer were mixed in a microplate. Then, 5 μL of caspase-1 fluorogenic substrate (WEHD-AFC) was added to initiate the reaction. After a 2-h reaction at 37 °C, the plates were read at excitation 400 nm and emission 505 nm in LS 55 florescence plate reader (PerkinElmer, Waltham, MA, USA). The results are expressed as the fold change in caspase-1 activity.[28]

Expression of IL-1β by real-time PCR

TRI reagent was used to extract total RNA from THP1 cells, and real-time PCR (RT-PCR) was performed for the quantitative analysis of IL-1β. From isolated RNA, 1 μg of RNA was used to synthesize cDNA by using a commercially available cDNA synthesis kit (RevertAid first stand DNA synthesis kit; Fermentas Life Sciences, Waltham, MA, USA). The volume of the reaction was 25 μL including Light Cycler 480 SYBR Green I Master (Roche Applied Science, Mannheim, Germany) and the following specific primers: IL-1β forward, 5′-CTCTCTCACCTCTCCTACTCAC-3′ and reverse, 5′-ACACTGCTACTTCTTGCCCC-3′; and β-actin forward, 5′-AACTGGAACGGTGAAGGTG-3′, and reverse, 5′-CTGTGTGGACTTGGGAGAGG-3′. This experiment was performed in a LightCycler 480 real-time PCR system (Roche Applied Science, Mannheim, Germany). To amplify the genes, a

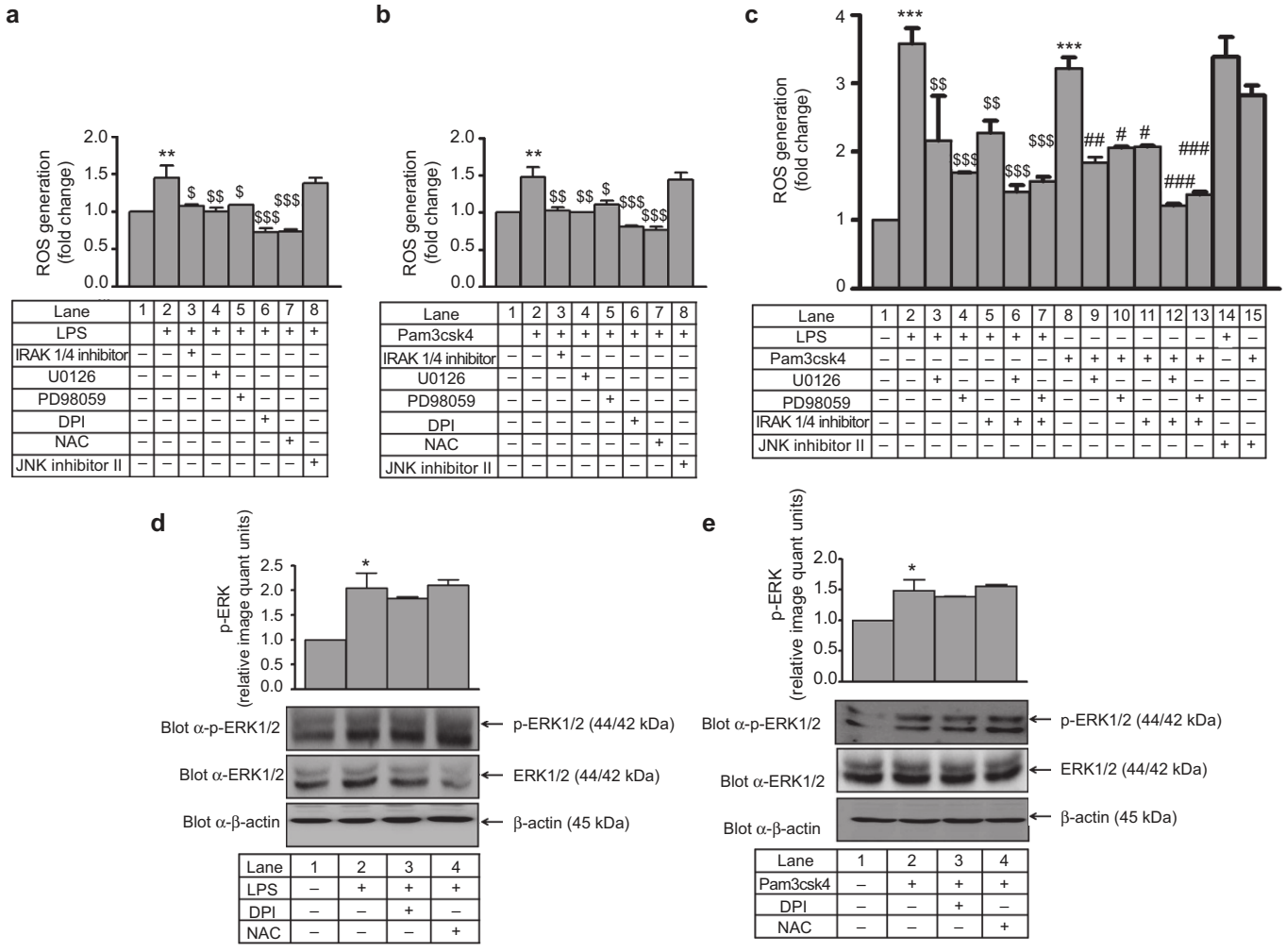

Figure 1 IRAK and ERK1/2 operate upstream of ROS during IL-1β production in THP-1 and primary human monocytes. IRAK1/4 inhibitor, U0126, PD98059, DPI, and NAC were used to pre-treat THP-1 cells that were then stimulated with (**a**) LPS and (**b**) Pam3csk4, and ROS generation was measured with DCF-DA. Fluorescence was measured with a microplate fluorimeter (in triplicate, $n = 3$). Similarly, primary human monocytes were pre-treated with an IRAK1/4 inhibitor or an ERK1/2 pathway inhibitor and stimulated with (**c**) LPS and Pam3csk4, and ROS generation was measured (in triplicate, $n = 3$). DPI and NAC pre-treated THP-1 cells were stimulated with (**d**) LPS and (**e**) Pam3csk4 for 30 min, and ERK1/2 phosphorylation was measured by western blotting ($n = 3$). Membranes were also probed with total ERK1/2 and β-actin Abs. The values represent the mean ± SE. $^{*}p < 0.05$, $^{**}p < 0.01$, $^{***}p < 0.001$ versus control; $^{\$}p < 0.05$, $^{\$\$}p < 0.01$, $^{\$\$\$}p < 0.001$ versus stimulated cells; $^{\#}p < 0.05$, $^{\#\#}p < 0.01$ $^{\#\#\#}p < 0.001$ versus Pam3csk4-stimulated cells.

three-step protocol was performed: an initial denaturation at 95 °C for 10 min; 35 cycles of 15-s denaturation at 95 °C and 30-s annealing at 60 °C; and a 30-s extension at 72 °C.[29] The comparative cycle threshold ($2^{-\Delta\Delta Ct}$) method was used to determine the relative fold difference between an experimental and calibrator sample. To calculate the relative expression, actin was used as housekeeping gene.[27]

Determination of intracellular ROS

To assess intracellular ROS generation, the cells were pre-treated with various inhibitors and then stimulated with LPS and Pam3csk4 for 1 h, and ROS generation was assessed using the oxidant-sensitive probes 2′,7′-dichlorofluorescein diacetate (H2DCF-DA,10 μmol L^{-1}, Sigma-Aldrich, St. Louis, MO, USA). H2DCF-DA was added to cultures 30 min before the end of the incubation. Fluorescence was measured at excitation 480 nm and emission 530 nm for H2DCF-DA with a microplate fluorimeter (BMG Labtech, Offenburg, Germany).[5]

Preparation of cytosolic and membrane fractions

For the preparation of cytosolic and membrane fraction, cells (5×10^7) were resuspended in relaxation buffer (KCl 100 mM; NaCl 3 mM; $MgCl_2$ 3.5 mM; EGTA 1.25 mM; EDTA 1 mM; NaF 10 mM; PMSF 1 mM; PIPES 10 mM; pH 7.3; Na_3VO_4 2 mM; pepstatin 20 lg mL^{-1}; trypsin inhibitor 20 lg mL^{-1}), sonicated and centrifuged at 500*g* for 10 min at 4 °C. Before undergoing ultracentrifugation, the supernatants were centrifuged twice at 10 000*g* for 5 min at 4 °C. Then, to obtain the

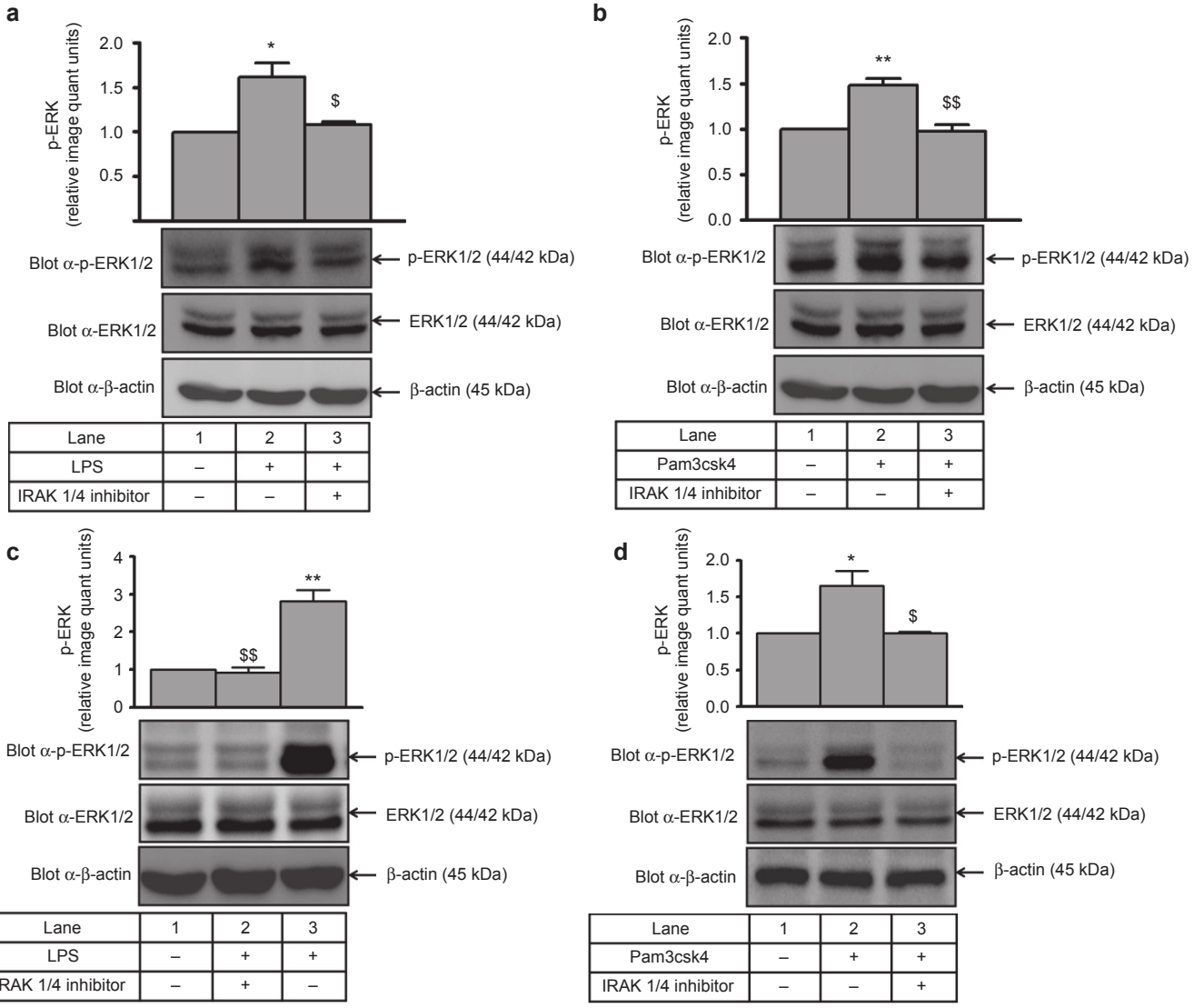

Figure 2 IRAK operates upstream of ERK1/2 during IL-1β production. THP-1 cells pre-treated with an IRAK1/4 inhibitor (0.3 μmol L^{-1}) were harvested after 30 min of (**a**) LPS or (**b**) Pam3csk4 treatment and processed for ERK1/2 activation. ERK1/2 phosphorylation was measured by immunoblotting with a p-ERK1/2 Ab ($n = 3$). ERK1/2 activation was also measured in primary human monocytes after pre-treatment with IRAK1/4 inhibitor and stimulation with (**c**) LPS and (**d**) Pam3csk4 for 30 min. The blots represent one of the three similar experiments. The values represent the mean ± SE. *$p < 0.05$, **$p < 0.01$ versus control; $^{\$}p < 0.05$, $^{\$\$}p < 0.01$ versus stimulated cells.

cytosolic and membrane fractions, ultracentrifugation was performed at 100 000*g* for 30 min at 4 °C. Then, the membrane fraction was washed with lysis buffer and then again centrifuged at 100 000*g* for 15 min and dissolved in lysis buffer containing 1% Triton X-100.[30]

Statistical analysis

The results are expressed as the mean ± SE. To calculate significant difference between two groups, unpaired Student's *t*-test was used. Comparisons were performed by one-way analysis of variance or by a Bonferroni multiple comparison test (GraphPad Prism, Demo, Version 5, GraphPad Software 2236 Avenida de la Playa La Jolla, CA, USA) for multiple comparisons of three or more groups. The differences were considered significant with a p value < 0.05. The blots represent one of the three or more comparable experiments.

RESULTS

IRAK1- and ERK1/2-dependent ROS generation and IL-1β production in THP-1 and primary monocytes

ROS was measured by DCF-DA after various interventions in THP-1. LPS- and Pam3csk4-induced ROS generation was significantly decreased (~1.5-fold) by IRAK1/4 inhibitor, U0126 and PD98059 (Figure 1a and 1b). In primary human monocytes, LPS- and Pam3csk4-induced ROS generation was significantly higher (~3-fold) compared with THP-1, and this effect was significantly decreased by IRAK1/4 inhibitor, U0126, and PD98059 (Figure 1c). A decrease (not significant) in ROS generation was observed when both IRAK1 and ERK1/2 pathway inhibitors were used in combination compared with individual treatments (Figure 1c). However, there was no significant inhibition in LPS- and Pam3csk4-induced ROS generation in JNK inhibitor II pre-treated THP-1 and primary monocytes. The significant increase in ERK phosphorylation observed after TLR4 and TLR2 stimulation was unaffected by DPI and NAC (Figure 1d and 1e) suggesting that ERK is upstream of ROS in the present experimental settings. In the present study, THP-1 cells treated with LPS (100 ng mL^{-1}) or Pam3csk4 (100 ng mL^{-1}) induced time-dependent ERK phosphorylation (Supplementary Figure S3a and S3b). In addition, LPS- and Pam3csk4-induced IL-1β production was significantly decreased (6.8-fold and 3.8-fold, respectively; $p < 0.001$) in the presence of U0126, PD98059, DPI, and NAC in THP-1 cells (Supplementary Figure S3c and S3d). LPS and Pam3csk4 also induced IL-1β production (4-fold and 3-fold, respectively) in primary human monocytes, and this effect was significantly decreased in U0126 and PD98059 pre-treated cells (Supplementary Figure S3e).

Regulation of ERK1/2 by IRAK1 during secretory IL-1β production

LPS- and Pam3csk4-induced ERK1/2 phosphorylation (1.5-fold increase; Figure 2a and 2b) was significantly decreased by the IRAK1/4 inhibitor (Figure 2a and 2b), suggesting that IRAK1 is upstream of ERK during IL-1β production. Similarly, in primary human monocytes, LPS- and Pam3csk4-induced ERK1/2 phosphorylation (~2.8- and 1.6-fold, respectively) was significantly abrogated by the IRAK1/4 inhibitor (Figure 2c and 2d).

To ascertain whether the change in ERK1/2 phosphorylation was accompanied by a change in its activity, a non-radioactive kinase assay was performed. LPS- and Pam3csk4-induced ERK1/2 activity (2 to 3 fold) was significantly inhibited (approximately 50%) in the presence of the IRAK1/4 inhibitor (Figure 3a and 3b). In primary human monocytes, LPS- and Pam3csk4-induced ERK1/2 activity (2.7- and 1.7-fold, respectively) was also abrogated by the IRAK1/4 inhibitor (Figure 3c). To further confirm the specificity of IRAK1-ERK1/2 regulation, siRNA-mediated gene silencing was performed. A significant reduction in IRAK1 and IRAK4 expression (Supplementary Figure S4a–d) and LPS- and Pam3csk4-induced ERK activity

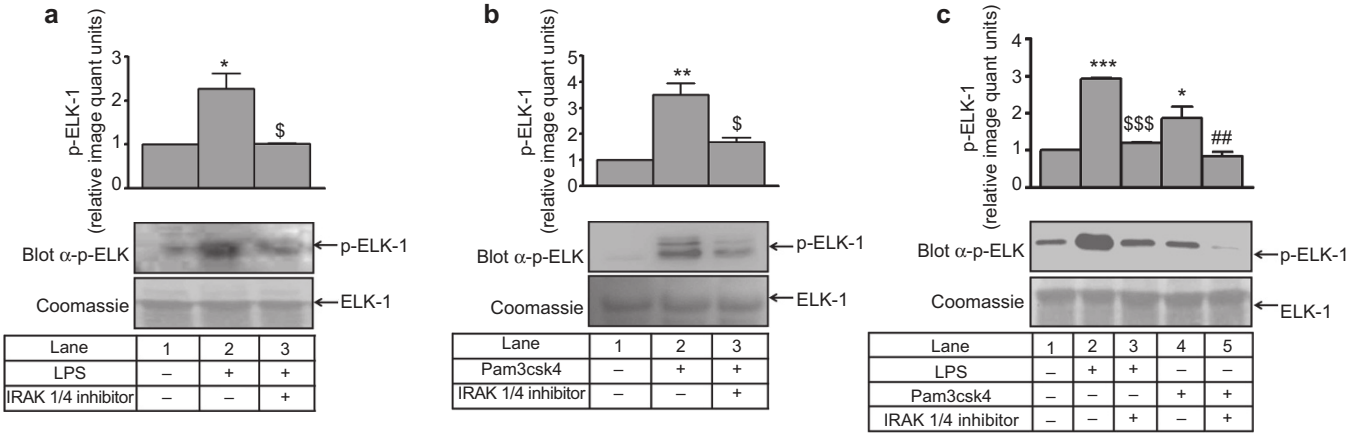

Figure 3 IRAK regulates ERK1/2 kinase activity during IL-1β production. THP-1 cells were harvested after pre-treatment with an IRAK1/4 inhibitor and 30 min of (**a**) LPS and (**b**) Pam3csk4 stimulation for ERK1/2 activity. Phosphorylation of the substrate was detected using a p-Elk-1 Ab ($n = 3$). ERK1/2 activity was also measured in primary human monocytes after IRAK1/4 inhibitor pre-treatment and (**c**) LPS and Pam3csk4 stimulation. The blots represent one of the three similar experiments. The values represent the mean ± SE. $^{*}p < 0.05$, $^{**}p < 0.01$, $^{***}p < 0.001$ versus control; $^{\$}p < 0.05$, $^{\$\$\$}p < 0.001$ versus stimulated cells; $^{\#\#}p < 0.01$ versus Pam3csk4-stimulated cells.

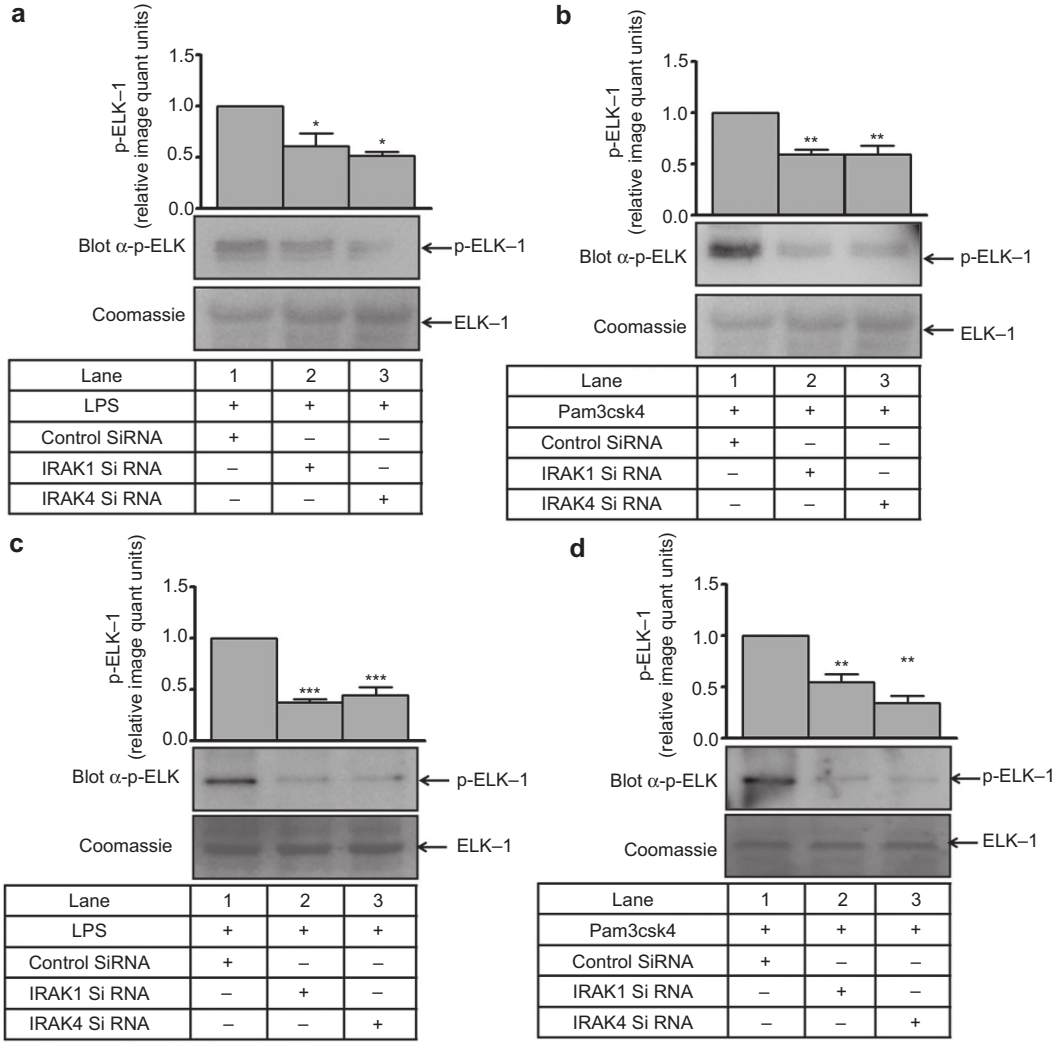

Figure 4 IRAK is upstream of ERK1/2 during IL-1β production. ERK1/2 activity was evaluated in (**a**) LPS- and (**b**) Pam3csk4-stimulated THP-1 cells that were transfected with control or IRAK1/4 siRNA ($n = 3$). Similarly, ERK1/2 activity was also evaluated in (**c**) LPS- and (**d**) Pam3csk4-stimulated primary human monocytes that were transfected with control or IRAK1/4 SiRNA ($n = 3$). The blots represent one of the three similar experiments. The values represent the mean ± SE. *$p < 0.05$, **$p < 0.01$, ***$p < 0.001$ versus control siRNA-transfected cells.

was observed in siRNA-treated cells (Figure 4a and 4b). Similar to THP-1, a significant reduction in IRAK1 and IRAK4 expression (Supplementary Figure S5a–d) and LPS- and Pam3csk4-induced ERK activity ($p < 0.001$) was observed in siRNA-treated cells (Figure 4c–d), thus confirming the role of IRAK1 and 4 in regulating ERK1/2 activation.

To evaluate any physical association between IRAK1 with ERK1/2, interaction studies were performed. ERK1/2 was detected in a complex immunoprecipitated by an anti (α) IRAK1 Ab. A significant increase in IRAK1–ERK1/2 interaction was observed in THP-1 upon LPS (1.6-fold) and Pam3csk4 (2-fold) treatment, which was significantly decreased by the IRAK1/4 inhibitor (Figure 5a). In primary human monocytes, LPS and Pam3csk4 induced the IRAK1–ERK1/2 interaction (2.8-fold, 2.1-fold, respectively), which was decreased ($p < 0.001$) in the presence of the IRAK1/4 inhibitor (Figure 5b). However, a negligible interaction was observed with isotype IgG in both cases. To ascertain whether the IRAK–ERK interaction was specific, reverse immunoprecipitation was performed by anti-ERK1/2 and IgG in LPS- and Pam3csk4-stimulated conditions. Again, a significant decrease in LPS- and Pam3csk4-stimulated IRAK–ERK interaction was obtained in THP-1 (Figure 5c) and monocytes (Figure 5d), and there was a negligible interaction in isotype IgG even in LPS- and Pam3csk4-stimulated conditions.

Role of IRAK1-ERK-ROS axis in AP-1-mediated IL-1β transcription

It is well established that AP-1 is downstream of JNK[31] and plays an important role in PMA-induced and IRAK1-mediated IL-1β transcription.[27] LPS- and Pam3csk4-induced IL-1β transcription was significantly inhibited by the AP-1 inhibitor tanshinone IIa, suggesting AP-1-dependent IL-1β transcription in THP-1 cells (Figure 6a).

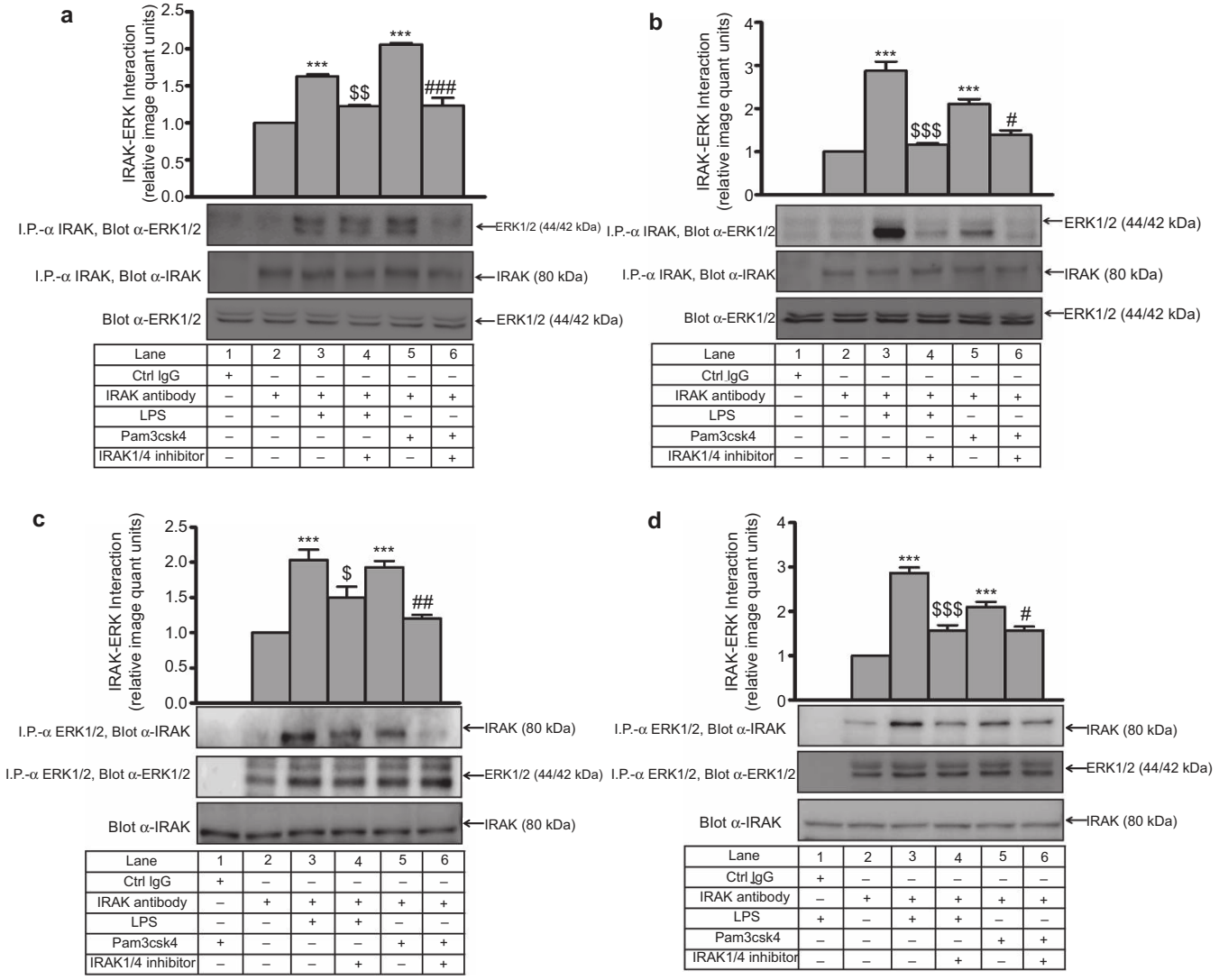

Figure 5 TLR induced IRAK1-dependent IRAK–ERK interaction. IRAK1/4 inhibitor pre-treated (**a**) THP-1 and (**b**) primary human monocytes were stimulated with LPS and Pam3csk4 for 30 min. IRAK and ERK1/2 interaction was assessed after immunoprecipitation with anti-IRAK-1 or the corresponding IgG isotype and immunoblotting with anti-ERK1/2 ($n = 3$). The IRAK and ERK1/2 interaction was also assessed after immunoprecipitation with anti-ERK1/2 or the corresponding IgG isotype and immunoblotting with anti-IRAK-1 in IRAK1/4 inhibitor-pre-treated (**c**) THP-1 and (**d**) primary human monocytes stimulated with LPS and Pam3csk4 for 30 min ($n = 3$). The blots represent one of the three similar experiments. The values represent the mean ± SE. ***$p < 0.001$ versus control; $^{\$}p < 0.05$, $^{\$\$}p < 0.01$, $^{\$\$\$}p < 0.001$ versus LPS; $^{\#}p < 0.05$, $^{\#\#}p < 0.01$, $^{\#\#\#}p < 0.001$ versus Pam3csk4-stimulated cells.

Moreover, LPS (Supplementary Figure S6a) and Pam3csk4 (Supplementary Figure S6b) also induced time-dependent JNK1/2 activation. Next, we explored whether there was a link between ERK and JNK during LPS- and Pam3csk4-induced IL-1β production. The initial JNK activation at 5 min and 15 min was not altered in the presence of U1026. However, LPS- (Figure 6b) and Pam3csk4- (Figure 6c) induced JNK phosphorylation was significantly inhibited at 30 min, 1 h, 6 h, and 12 h in the presence of U0126. These data suggest that there may be two phases of JNK activation; ERK may affect only the later phase, or sustained JNK activation may require ERK.

To test whether ROS can induce the JNK-AP-1 axis during IL-1β transcription, p-JNK was monitored in the presence of DPI and NAC. A significant increase (~2-fold) in JNK1/2 phosphorylation was observed after LPS and Pam3csk4 treatment. This increase in phosphorylation significantly decreased with DPI and NAC (Figure 7a and 7b), indicating ROS-dependent JNK1/2 activation. Moreover, LPS- and Pam3csk4-induced AP-1 activation (~5-fold and ~4-fold, respectively) in THP-1 was significantly reduced in the presence of IRAK1/4 inhibitor, U0126, PD98059, DPI, and NAC (Figure 7c–d) thus indicating IRAK1-, ERK1/2-, and ROS-dependent AP-1 activation. Similar to THP-1, in human monocytes, LPS- and Pam3csk4-induced AP-1 activation (~6.5-fold and ~7.2-fold, respectively) was significantly decreased with the IRAK1/4 inhibitor and U0126 (Supplementary Figure S7a). In addition, LPS- and Pam3csk4-induced JNK1/2 activation (3.4-fold and

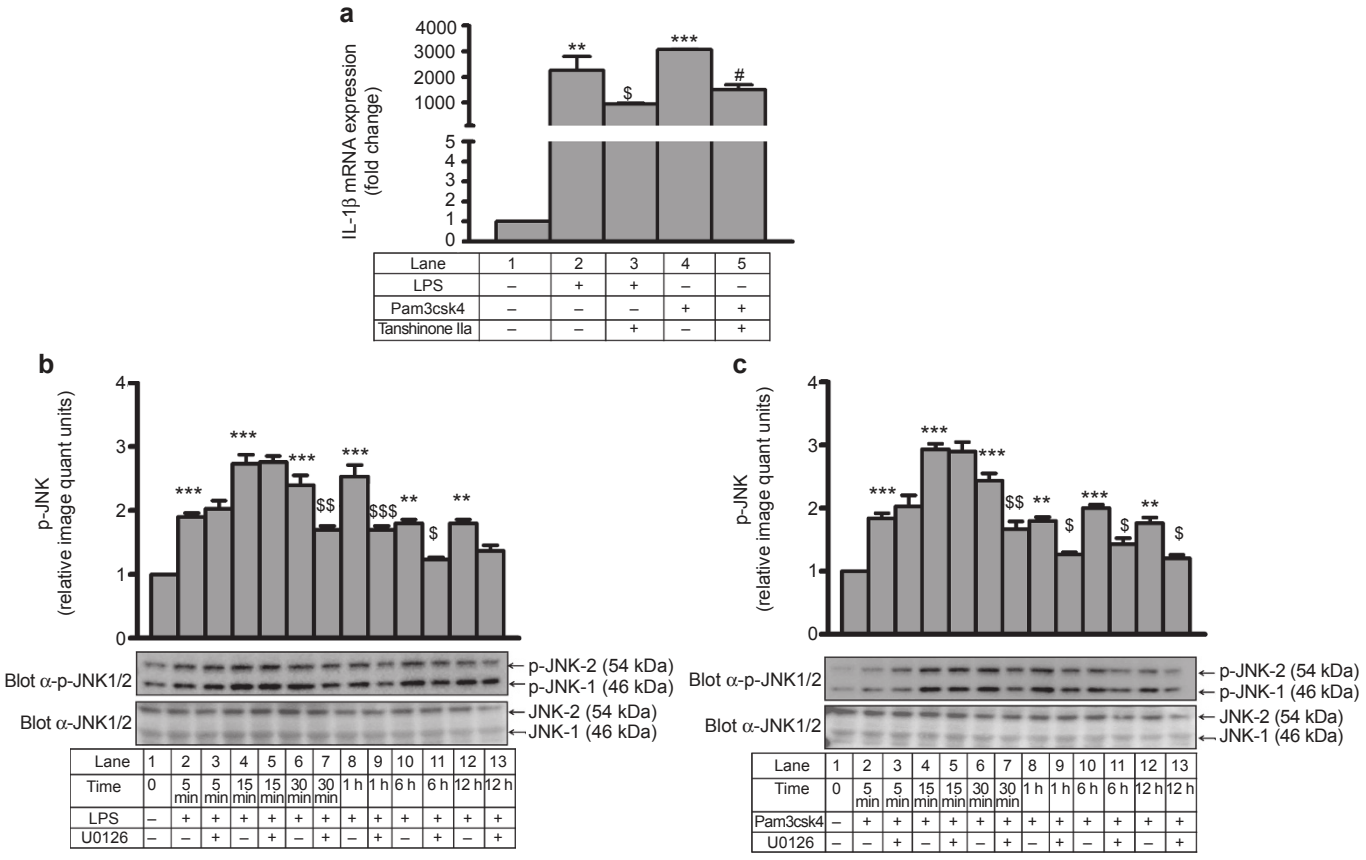

Figure 6 AP-1-dependent IL-1β transcription and ERK1/2-mediated JNK activation. (**a**) Tanshinone IIa pre-treated THP-1 cells were stimulated with LPS and Pam3csk4 for 24 h, and IL-1β mRNA was measured by quantitative RT-PCR ($n = 3$). Time response of JNK activation was monitored with and without U0126 after (**b**) LPS and (**c**) Pam3csk4 stimulation. Membranes were also probed with total JNK1/2 Ab ($n = 3$). The values represent the mean ± SE. $^{**}p < 0.01$, $^{***}p < 0.001$ versus control; $^{\$}p < 0.05$, $^{\$\$}p < 0.01$, $^{\$\$\$}p < 0.001$ versus stimulated cells; $^{\#}p < 0.05$ versus Pam3csk4-stimulated cells.

3.3-fold, respectively; Supplementary Figure S7b–c) was significantly inhibited with the IRAK1/4 inhibitor and the ERK pathway inhibitor ($p < 0.01$). In the present study, LPS- and Pam3csk4-induced IL-1β transcription (~4000-fold and ~3000 fold, respectively) was significantly reduced ($p < 0.001$) in the presence of IRAK1/4 inhibitor, U0126, PD98059, DPI, and NAC (Supplementary Figure S8a and S8b).

Role of IRAK in ERK1/2-induced p67phox activation in THP-1

To delineate the underlying mechanism by which IRAK and ERK1/2 could modulate NADPH oxidase, we examined whether endogenous ERK1/2 and p67phox interact with each other by immunoprecipitation with anti-ERK1/2 and immunoblotting with an anti-p67phox Ab. LPS (2-fold) and Pam3csk4 (2.7-fold) induced the ERK1/2–p67phox association. This physical interaction was decreased significantly in IRAK1/4 inhibitor pre-treated and LPS- and Pam3csk4-stimulated cells ($p < 0.01$, $p < 0.001$, respectively; Figure 8a and 8b). However, a negligible interaction was observed with isotype IgG. In a reverse immunoprecipitation experiment, ERK1/2 was detected in a complex immunoprecipitated with an anti-p67phox Ab; similar results were obtained (Figure 8c).

For analyzing p67phox activation, we monitored its translocation to the membrane after agonist stimulation. There was significant increase in the membrane translocation of p67phox from the cytoplasm upon LPS ($p < 0.01$) and Pam3csk4 ($p < 0.001$) challenge, and this translocation was significantly inhibited by the IRAK1/4 inhibitor and U0126 (Figure 8d and 8e). There was negligible amount of p67phox in the membrane fraction in control cells. p67phox can complex with several Nox isoforms, including Nox-2 and Nox-1, during NADPH oxidase complex activation and ROS production.[32] Therefore, the p67phox–Nox-2 interaction was examined by immunoprecipitation with anti-Nox-2 and immunoblotting with an anti-p67phox Ab. LPS- (2.3-fold) and Pam3csk4- (2.1-fold) induced p67phox–Nox-2 interaction was significantly attenuated with IRAK and ERK pathway inhibitors (Figure 9a and 9b). We also observed that TLR2 and TLR4 induced p47phox phosphorylation in an ERK-dependent manner (Supplementary Figure S9).

TLR4 and TLR2 mediate LPS- and Pam3csk4-induced IRAK-ERK-ROS regulation and IL-1β production

THP-1 cells transfected with TLR4 siRNA or TLR2 siRNA and stimulated with LPS or Pam3csk4, respectively, were found to

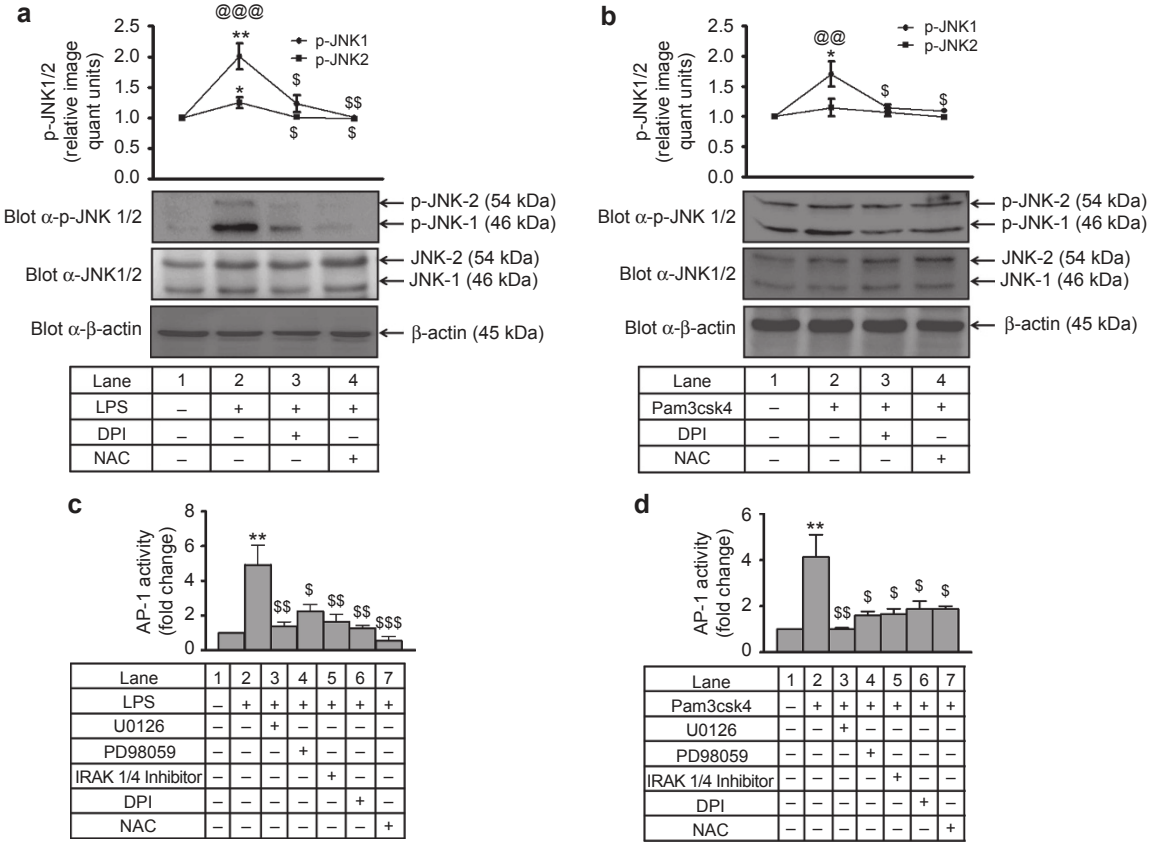

Figure 7 IRAK, ERK and ROS mediate LPS- and Pam3csk4-induced AP-1 activation in THP-1. DPI and NAC pre-treated THP-1 cells were stimulated with (**a**) LPS and (**b**) Pam3csk4 for 30 min, and JNK activation was measured by probing the blots with p-JNK Ab. Membranes were also probed with total JNK1/2 and β-actin Abs ($n = 3$). THP-1 cells pre-treated with inhibitors of specific pathways were stimulated with (**c**) LPS and (**d**) Pam3csk4 for 30 min, and AP-1 activity was measured in nuclear extracts by using a TransAM Ap-1-c-jun kit ($n = 3$). The values represent the mean ± SE. $^{*}p < 0.05$, $^{**}p < 0.01$, versus control; $^{\$}p < 0.05$, $^{\$\$}p < 0.01$, $^{\$\$\$}p < 0.001$ versus stimulated cells; $^{@@}p < 0.01$, $^{@@@}p < 0.001$ JNK1 versus JNK2.

have significantly reduced levels of ROS generation (23% and 30%, respectively; Figure 10a) and secreted IL-1β ($p < 0.05$; Figure 10b) compared with control siRNA-transfected cells. The LPS- and Pam3csk4-induced IRAK–ERK interaction was also significantly reduced ($p < 0.001$) in TLR4 siRNA- and TLR2 siRNA-transfected cells compared with those transfected with scrambled siRNA (Figure 10c). In accordance with this result, LPS- and Pam3csk4-induced ERK–p67phox interaction was also significantly inhibited when transfected with TLR4 siRNA ($p < 0.01$) or TLR2 siRNA ($p < 0.05$) compared with control siRNA-transfected cells (Figure 10d). A significant decrease in TLR4 and TLR2 ($p < 0.01$) expression was observed after transfection of the corresponding siRNA (Supplementary Figure S10a and S10b).

Role of IRAK-ERK-ROS axis in IL-1β processing

Interestingly, not only IL-1β transcription but also IL-1β processing was affected by IRAK, ERK and ROS. LPS- and Pam3csk4-induced caspase-1 activation (~2-fold) was significantly inhibited in the presence of U0126, PD98059, DPI, and NAC (Figure 11a). Similarly, in primary human monocytes, LPS- and Pam3csk4-induced (Figure 11b and 11c, respectively) caspase-1 activity (~2.5-fold) was dependent on ERK1/2 and ROS. Treatment with the IRAK1/4 inhibitor significantly reduced (~24%) LPS- and Pam3csk4-induced caspase 1 activity (Supplementary Figure S11a) and IL-1β processing (Supplementary Figure S11b). In addition, transfection of IRAK-1 siRNA also significantly reduced (20%) LPS- and Pam3csk4-induced caspase-1 activity (Supplementary Figure S11c).

The role of ERK1/2 and ROS in IL-1β processing was further assessed by evaluating the expression of intracellular pro-IL-1β and IL-1β. LPS- and Pam3csk4-induced pro-IL-1β (~4.0-fold) and IL-1β (~2.5-fold) expression (Figure 11d and 11e). This increase in expression of pro-IL-1β and IL-1β was significantly ($p < 0.001$) reduced in the presence of U0126, PD98059, DPI, and NAC.

Nox-2 dependent IL-1β transcription, processing, and secretion in THP-1 and primary monocytes

Next, the role of Nox-2 was examined in LPS- and Pam3csk4-induced IL-1β secretion. Secretory IL-1β was also significantly inhibited with Nox-2 siRNA by 23% and 27% in LPS- and Pam3csk4-stimulated THP-1 monocytes, respectively, compared

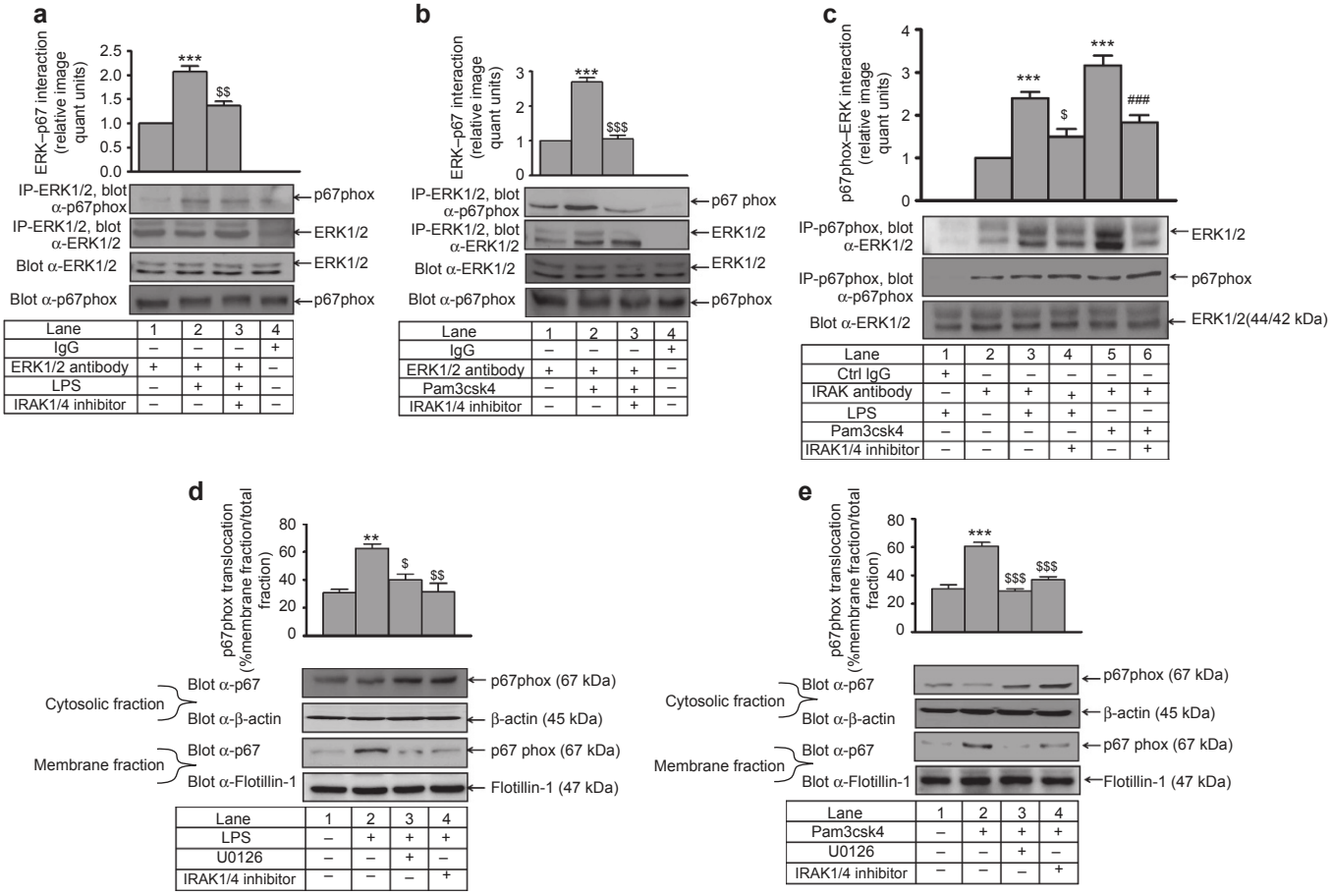

Figure 8 IRAK is required for LPS- and Pam3csk4-induced ERK1/2–p67phox interaction and p67phox membrane translocation. IRAK1/4 inhibitor pre-treated THP-1 monocytes were stimulated with (**a**) LPS and (**b**) Pam3csk4 for 30 min. Endogenous ERK1/2 and p67phox interaction was assessed after immunoprecipitation with anti-ERK1/2 and corresponding IgG isotype and immunoblotting with anti-p67phox ($n = 3$) or (**c**) by immunoprecipitation with anti-p67phox Ab and immunoblotting with anti-ERK1/2. IRAK1/4 inhibitor and U0126 pre-treated THP-1 cells were stimulated with (**d**) LPS and (**e**) Pam3csk4 for 1 h. Cells were sonicated and fractionated into cytoplasmic and membrane fractions by ultracentrifugation. Both fractions were analyzed by immunoblotting with anti-p67phox Ab ($n = 3$). The blots represent one of the three similar experiments. The values represent the mean ± SE. $^{**}p < 0.01$, $^{***}p < 0.001$ versus control; $^{\$}p < 0.05$, $^{\$\$}p < 0.01$, $^{\$\$\$}p < 0.001$ versus stimulated cells; $^{\#\#\#}p < 0.001$ versus Pam3csk4-stimulated cells.

with control siRNA (Figure 12a). Moreover, an 80% and 68% decrease in IL-1β mRNA expression was observed in Nox-2 siRNA-treated cells that were stimulated with LPS and Pam3csk4, respectively, compared with their controls (Figure 12b). Not only transcription but also processing was Nox-2 dependent, as caspase-1 activity was inhibited (30% and 41% with LPS and Pam3csk4, respectively) in Nox-2 siRNA-treated cells (Figure 12c). LPS- and Pam3csk4-induced intracellular pro-IL-1β and mature IL-1β was also significantly attenuated ($p < 0.001$) with Nox-2 SiRNA (Figure 12d). Similarly, primary human monocytes transfected with Nox-2 siRNA secreted significantly lower levels of LPS- and Pam3csk4-induced IL-1β compared with control siRNA-transfected cells (Supplementary Figure S12a). Moreover, a significant decrease in IL-1β mRNA expression was observed in Nox-2 siRNA-treated ($p < 0.05$, $p < 0.01$) cells that were stimulated with LPS and Pam3csk4, respectively, compared with their controls (Supplementary Figure S12b). Not only transcription but also processing was Nox-2 dependent, as caspase 1 activity was inhibited ($p < 0.001$ and $p < 0.01$ with LPS and Pam3csk4, respectively) in Nox-2 siRNA-treated cells (Supplementary Figure S12c). A significant reduction in Nox-2 expression was observed after transfection of its siRNA (Supplementary Figure S12d and S12e). Moreover, IL-1β secretion in Nox-2 siRNA-transfected cells was also evaluated in the presence of a second stimulus, ATP, for inflammasome activation (Supplementary Figure S13). There was significant reduction in IL-1β secretion with Nox-2 siRNA-transfected and LPS/Pam3csk4- and ATP-stimulated cells compared with control siRNA-transfected cells (Supplementary Figure S13a). Moreover, there was significant reduction in Nox-2 protein expression in Nox-2 siRNA-transfected cells that were primed with LPS (Supplementary Figure S13b) and Pam3csk4 (Supplementary Figure S13c) and stimulated with ATP compared with control siRNA-transfected cells.

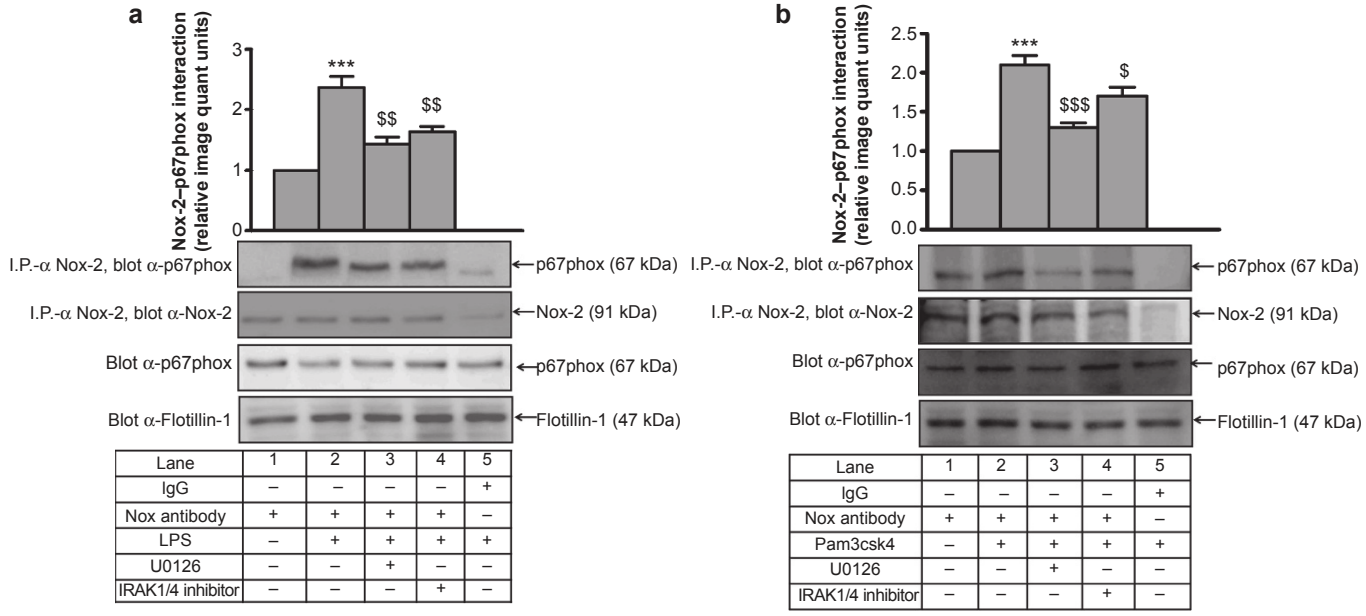

Figure 9 IRAK- and ERK1/2-dependent LPS- and Pam3csk4-induced p67phox–Nox-2 interaction. IRAK1/4 inhibitor and U0126 pre-treated THP-1 cells were stimulated with (**a**) LPS and (**b**) Pam3csk4 for 1 h, and the membrane fraction was isolated. Endogenous p67phox and Nox-2 interaction was assessed after immunoprecipitation with anti-Nox-2 and corresponding IgG isotype and immunoblotting with anti-p67phox ($n = 3$). The blots represent one of the three similar experiments. The values represent the mean ± SE. ***$p < 0.001$ versus control; $^{\$}p < 0.05$, $^{\$\$}p < 0.01$, $^{\$\$\$}p < 0.001$ versus stimulated cells.

DISCUSSION

We examined the regulation of TLR2- and TLR4-induced ROS generation and demonstrated its regulation by IRAK1, ERK1/2, p67phox, and Nox-2 during secretory IL-1β production, transcription and processing in THP-1 and primary human monocytes. It has been reported that targeting macrophage redox status may represent a promising therapy for human Type 1 diabetes.[33] For activation of TLR2 and TLR4, we used the TLR2-specific ligand Pam3csk4[34,35] and the TLR4-specific ligand LPS.[36] To ascertain whether the LPS- and Pam3csk4-induced effects observed in the present study were indeed mediated by TLR4 and TLR2, experiments were performed in the presence of receptor-specific siRNA. Pam3csk4- and LPS-induced effects were significantly blocked by TLR2 and TLR4 siRNA, respectively, demonstrating that the effects observed by the ligands were specific to their respective receptors. TLR2 and TLR4 interacts with Nox,[37] and their activation leads to Nox-2-dependent ROS generation. However, how IRAK regulates TLR-mediated Nox-2 activation for IL-1β secretion is not clear. IRAKs are key components in the signal transduction pathways of TLRs.[38] Moreover, the effect of Nox-2 on IL-1β transcription, processing and secretion has not been defined. Our findings connect TLR-induced signaling events with p67phox and Nox-2 mediated ROS generation for IL-1β production. It has been reported that TLR engagement activates NADPH oxidase and ROS production leading to the increased expression of inflammatory cytokines, including IL-1β.[39] However, the intermediary signaling cascade was not clear, and how individual components of NADPH oxidase complex modulated IL-1β production and to what level has not been determined. ERK1/2 regulation by ROS and vice versa is controversial[40,41] with no data on their inter-regulation for IL-1β production. Therefore, the present study was undertaken to address these issues.

In the present study, TLR2- and TLR4-induced IRAK1- and ERK1/2-mediated ROS generation in THP-1 and primary human monocytes. In primary human monocytes, a higher amount of ROS was generated compared with THP-1; therefore, higher levels of secretory IL-1β were observed in monocytes. It has already been reported that different myeloid cells display different redox status under resting conditions or upon TLR engagement.[42] Moreover, IRAK1 and ERK1/2 operate in the same pathway for ROS production, as inhibition by the combination of inhibitors was not significant compared with the effect of the individual inhibitors alone.

The inter-regulation of IRAK1 and ERK1/2 was investigated, as both of these kinases are activated during IL-1β production. Interestingly, it was found that IRAK induces ERK activity during TLR2- and TLR4-induced IL-1β production. Although there is a report suggesting that IRAK feeds into ERK pathway, there is no information regarding its impact on TLR-induced IL-1β production.[43] It has also been reported that there is a minimal effect of the IRAK1/4 inhibitor on ERK activation after R848 (TLR7/TLR8 ligand) stimulation.[11] Thus, it is possible that kinases other than IRAK1/4 also feed into the ERK pathway after R848 stimulation. Therefore, it was demonstrated for the first time that IRAK1/4 is upstream of ERK1/2 in the secretory IL-1β production pathway in monocytes. The present study indicates

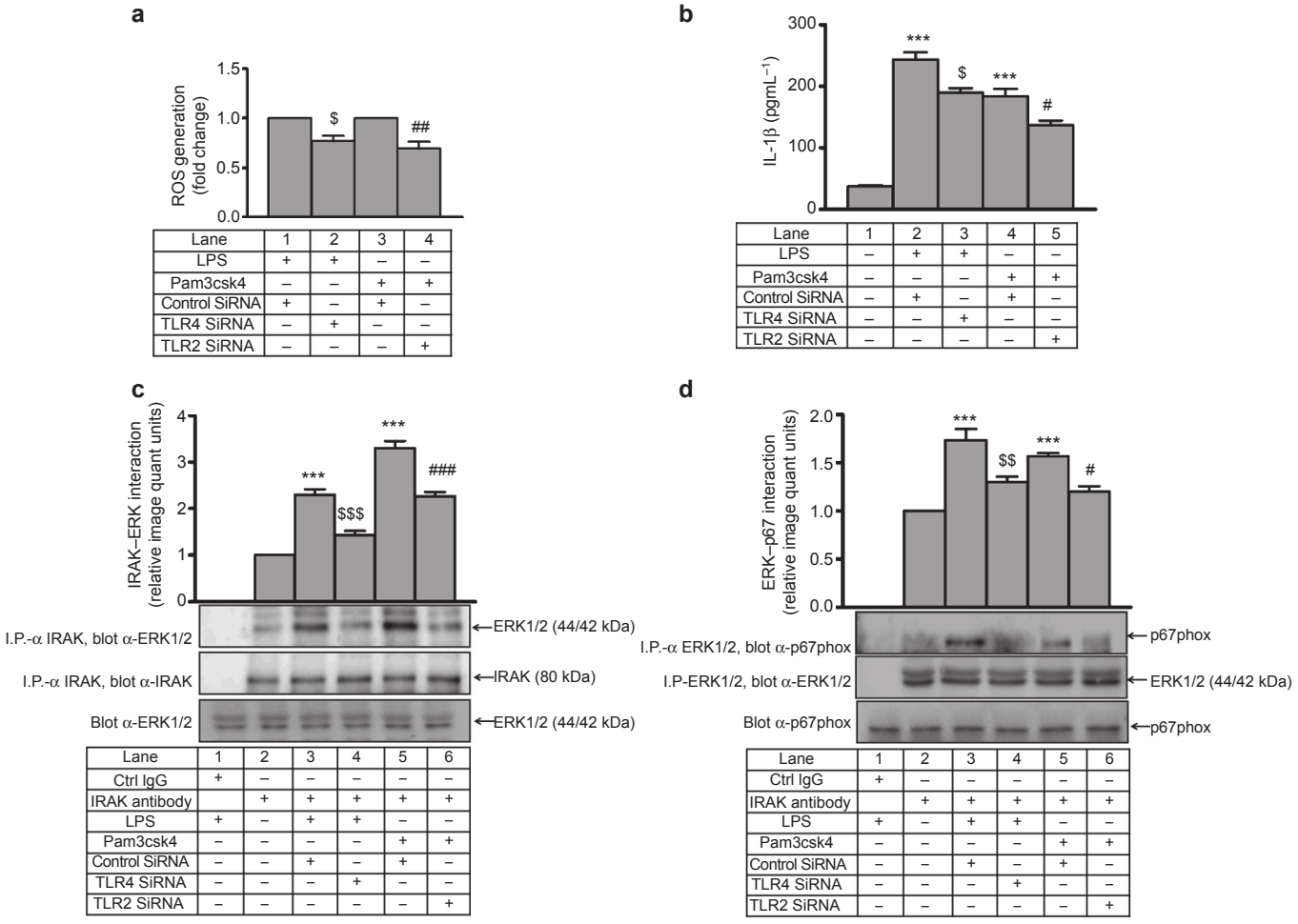

Figure 10 TLR4- and TLR2-mediated IL-1β secretion and IRAK-ERK-ROS regulation in THP-1. In THP-1 cells transfected with TLR4 siRNA or TLR2 siRNA and stimulated with LPS and Pam3csk4, respectively. (**a**) ROS generation was measured with DCF-DA and (**b**) IL-1β secretion was measured by ELISA. Similarly, THP-1 cells transfected with TLR4/TLR2 siRNA were stimulated with LPS and Pam3csk4 for 30 min, and (**c**) IRAK–ERK interaction was measured after immunoprecipitation with anti-IRAK-1 and corresponding IgG isotype and immunoblotting with anti-ERK1/2 ($n = 3$). (**d**) ERK–p67phox interaction was assessed after immunoprecipitation with anti-ERK1/2 or the corresponding IgG isotype and immunoblotting with anti-p67phox ($n = 3$). The blots represent one of the three similar experiments. The values represent the mean ± SE. $^{***}p < 0.001$ versus control; $^{\$}p < 0.05$, $^{\$\$}p < 0.01$, $^{\$\$\$}p < 0.001$ versus control SiRNA + LPS; $^{\#}p < 0.05$, $^{\#\#}p < 0.01$, $^{\#\#\#}p < 0.001$ versus control siRNA + Pam3csk4-transfected cells.

new methods of activating ERK after TLR stimulation. At the same time, there are other methods by which TLR-induced MAPK activation can occur, including activation via IκB kinase[44] and TLR-induced Ras/Raf activation leading to activation of MEK/ERK pathway.[45] In the present study, IRAK1 is not only upstream of ERK1/2 but also interacts with ERK1/2 and modulates its activity as demonstrated with interaction experiments. The kinase activity of IRAK is important for the association of IRAK1 and ERK1/2 because significant inhibition of the TLR2- and TLR4-induced IRAK–ERK interaction was observed with the IRAK1/4 inhibitor. In contrast, there was no significant difference in ERK phosphorylation in THP-1 cells transfected with pRK7IRAK (W/T) compared with myc-pRK7IRAK (K239S; data not shown). It is possible that the *in vivo* inhibition of both IRAK1 and IRAK4 kinase activity is important for observing a significant inhibition of ERK phosphorylation. In IRAK4 kinase-dead knock-in mice, there was severe impairment of MAPK activation and IL1/TLR-induced cytokine production.[46] It has been shown that mutation of critical threonine at position 209 (T209) completely abrogates IRAK1 kinase activity, suggesting its importance for IRAK1 activation.[47] Recently, an IRAK1 D359A-mutant, which is catalytically inactive, mouse has been reported.[48] In addition, for induction of IRAK-1 kinase activity, phosphorylation of Thr-387 in the IRAK-1 activation loop (amino acids 358-389) is critical.[49] In the present study, it was found that during TLR2 and TLR4 induced IL-1β production, ERK1/2 is upstream of ROS as there was no effect of DPI and NAC on ERK1/2 phosphorylation. Inhibition of TLR2- and TLR4-induced ROS generation with U0126, PD98059, and IRAK1/4 inhibitor further strengthens this claim.

LPS and Pam3csk4 caused prolonged JNK1/2 activation, and ERK was found to inhibit the late phase of JNK activation, as also noted by others in different systems.[50,51] We found that

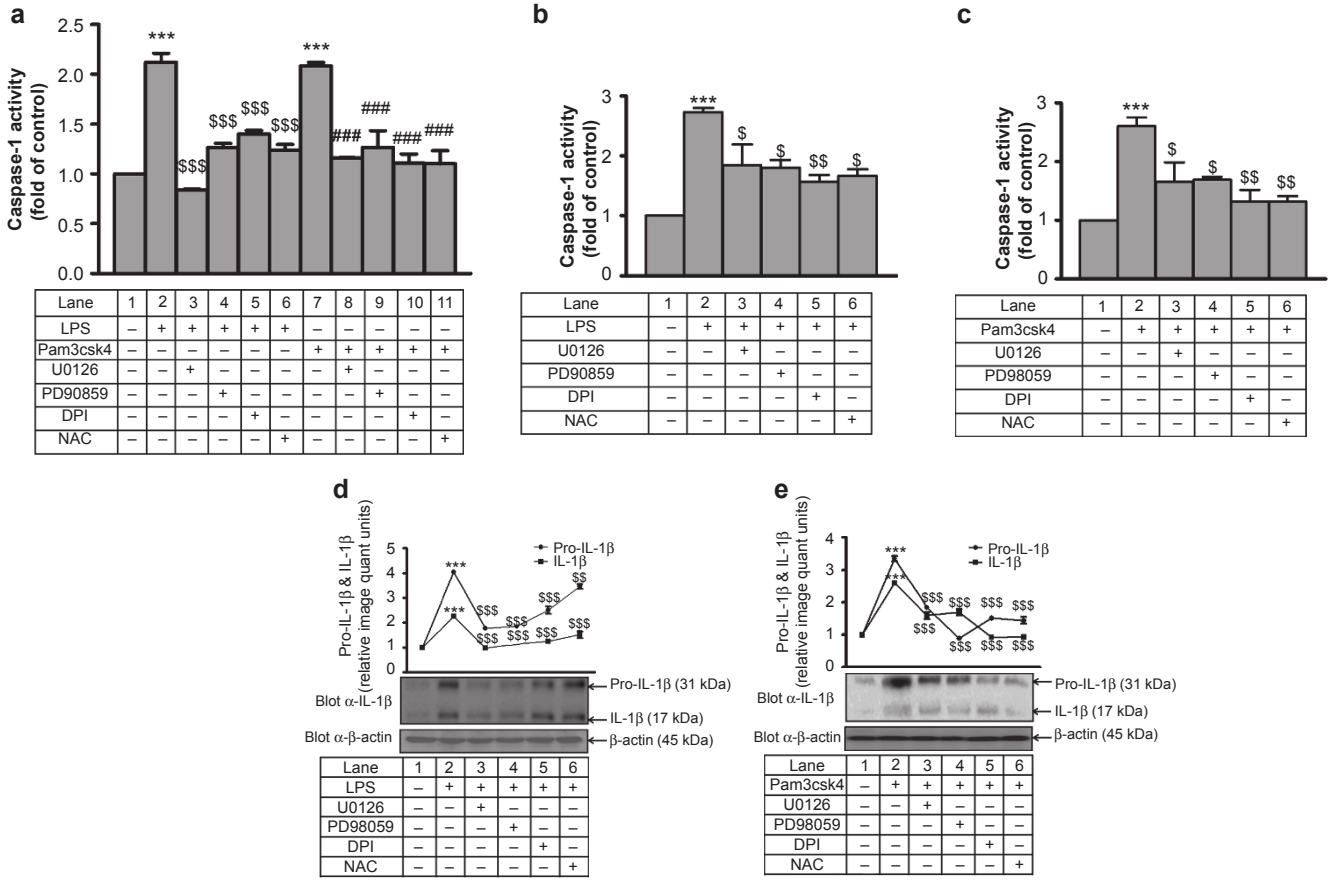

Figure 11 Role of ERK and ROS in LPS- and Pam3csk4-induced caspase-1 activation and IL-1β processing. Caspase-1 activity was measured by fluorometric assay in (**a**) THP-1 cells and (**b**–**c**) primary monocytes after U0126, PD98059, DPI, and NAC pre-treatment followed by stimulation with LPS and Pam3csk4 for 24 h ($n = 3$). U0126, PD98059, DPI, and NAC pre-treated THP-1 cells were stimulated with (**d**) LPS and (**e**) Pam3csk4 for 24 h, and pro-IL-1β and mature IL-1β protein expression was measured by western blotting ($n = 3$). The blots represent one of the three similar experiments. $^{***}p < 0.001$ versus control; $^{\$}p < 0.05$, $^{\$\$}p < 0.01$, $^{\$\$\$}p < 0.001$ versus stimulated cells; $^{\#\#\#}p < 0.001$ versus Pam3csk4-stimulated cells.

TLR2- and TLR4-induced IL-1β transcription in THP-1 was AP-1 mediated, and there was ROS-dependent JNK1/2 activation. AP-1 activity and IL-1β transcript levels were significantly reduced in the presence of IRAK1/4 inhibitor, U0126, PD98059, DPI, and NAC, indicating that IRAK-ERK-ROS operated upstream of the JNK1-AP-1 axis during TLR2- and TLR4-induced IL-1β transcription. However, the IL-1β gene contains binding motifs for several other transcription factors, such as nuclear factor-κB/Rel, AP-1, NF-IL6, and cyclic AMP-responsive element binding protein/activation transcriptional factor (CREB/ATF), which appear to be important in LPS-mediated IL-1β induction.[52] CREB can also contribute to LPS- and Pam3csk4-induced IL-1β production because we also observed ERK-dependent LPS- and Pam3csk4-induced CREB phosphorylation (data not shown).

The production of IL-1β involves the transcription of pro IL-1β, then cleavage of pro IL-1β into IL-1β by caspase-1.[6] IRAK-, ERK1/2-, and ROS-dependent caspase-1 activation was observed in THP-1 and primary human monocytes. It has also been reported that ATP-dependent ROS production and ERK1/2 activation are upstream of caspase-1 activation.[53] Some reports suggest that deletion of IRAK1 or IRAK4 leads to defective inflammasome activation.[54] In accordance with this suggestion, we also observed significantly less caspase-1 activity after treatment with IRAK1 siRNA or an IRAK1/4 inhibitor. Abrogation of kinase activity of IRAK-1 does not completely prevent rapid inflammasome activation, suggesting that IRAK-1 might have additional kinase-independent functions that regulate NLRP3 inflammasome activation.[55] The fold increase in caspase-1 activity was very similar in THP-1 and monocytes; however, basal caspase-1 activity was higher in monocytes, indicating that higher ROS leads to increased caspase-1 activity and IL-1β production. Intracellular pro IL-1β and mature IL-1β expression after stimulation was reduced in the presence of IRAK1/4 inhibitor, U0126, PD98059, DPI, and NAC, further confirming the role of IRAK, ERK1/2, and ROS in IL-1β processing.

TLR2- and TLR4-induced NADPH oxidase activation because the translocation of p67phox to membrane and p47phox phosphorylation was observed upon stimulation. In

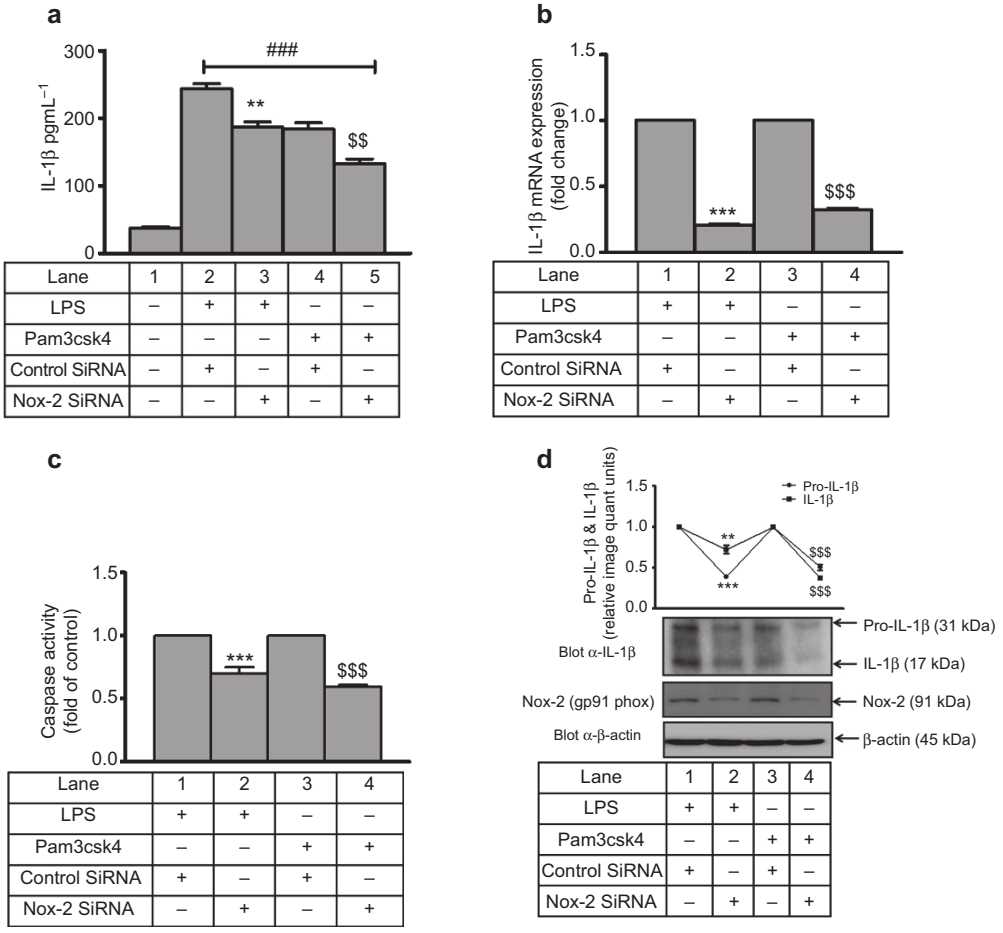

Figure 12 Nox-2-dependent IL-1β secretion, transcription and processing in THP-1. Nox-2 and control siRNA-transfected THP-1 cells were stimulated with LPS and Pam3csk4 for 24 h, and (**a**) IL-1β secretion, (**b**) IL-1β mRNA expression, (**c**) caspase-1 activity, and (**d**) pro-IL-1β and mature IL-1β expression was measured. Nox-2 expression was also analyzed by western blotting. The values represent the mean ± SE. $^{###}p < 0.001$ versus control, $^{**}p < 0.01$, $^{***}p < 0.001$ versus control siRNA + LPS, $^{\$\$}p < 0.01$, $^{\$\$\$}p < 0.001$ versus control siRNA + Pam3csk4-stimulated cells.

monocytes, upon NADPH oxidase complex activation, the cytosolic components (p47phox, p67phox) translocate to the membrane and actively catalyzes the production of superoxide anion.[56] TLR2- and TLR4-induced IRAK1 regulates ROS generation by regulating the ERK–p67phox interaction because in presence of an IRAK1/4 inhibitor, decreased ERK–p67phox interaction is observed, resulting in reduced translocation of p67phox to the membrane. Using a specialized program,[57] an in silico-based phosphorylation site analysis was performed. The presence of putative high stringency ERK-binding site (V403) in p67phox (analysis not shown) was found. This result may explain the binding of p67phox with ERK. However, whether interruption of the putative ERK binding motif in p67phox abolishes ERK/p67phox interaction and ROS generation requires experimental validation. p67phox can complex with Nox-1, Nox-2, and Nox-3 during superoxide production.[32] In the present study, TLR4- and TLR2-mediated p67phox–Nox-2 interaction was IRAK and ERK dependent. It has been reported that diabetic mice deficient in Nox-derived ROS were protected due to blunted TLR-dependent macrophage responses.[33] Because Nox-2 is the major isoform present in monocytes, we evaluated its role in IL-1β production. The role of Nox-2 in IL-1β secretion, transcription and processing was evident by siRNA experiments. Nox-2 is essential for TLR2-induced inflammatory response in macrophages[37] and TLR4 activation appears to be a prerequisite for Nox-2 activation.[58] Based on these results, it can be asserted that, at least, Nox-2 plays a significant role in TLR2- and 4-induced IL-1β production, transcription, and processing. The present study thus connects the TLR pathway with the ERK-p67phox-Nox-2 axis for IL-1β production, transcription, and processing in monocytic cells. Whether other Nox isoforms, such as Nox-1 and Nox-4, also operate in a similar manner requires further investigation.

We propose a novel pathway in which TLR2 and TLR4 induce IRAK1-ERK activation, which subsequently regulates the ERK–p67phox interaction and Nox-2-dependent ROS generation for IL-1β transcription and processing in an AP-1- and caspase-1-dependent manner.

COMPETING INTERESTS

The authors declare no commercial or financial conflict of interest.

ACKNOWLEDGEMENTS

The authors gratefully acknowledge the technical help provided by Mr. C.P. Pandey, Mrs. M. Chaturvedi, and Mr. A.L. Vishwakarma. Funding from THUNDER BSC0102 CSIR Network project to Manoj Kumar Barthwal is gratefully acknowledged. Fellowships from University Grants Commission to Ankita Singh and Council of Scientific and Industrial Research to Vishal Singh and Rajiv L Tiwari are acknowledged. CDRI communication number: 9008.

Supplementary information of this article can be found on *Cellular & Molecular Immunology* website: http://www.nature.com/cmi.

1 Lavieri R, Piccioli P, Carta S, Delfino L, Castellani P, Rubartelli A. TLR costimulation causes oxidative stress with unbalance of proinflammatory and anti-inflammatory cytokine production. *J Immunol* 2014; **192**: 5373–5381.
2 Lucas K, Maes M. Role of the Toll like receptor (TLR) radical cycle in chronic inflammation: possible treatments targeting the TLR4 pathway. *Mol Neurobiol* 2013; **48**: 190–204.
3 Chandra R, Federici S, Bishwas T, Nemeth ZH, Deitch EA, Thomas JA *et al.* IRAK1-dependent signaling mediates mortality in polymicrobial sepsis. *Inflammation* 2013; **36**: 1503–1512.
4 Dinarello CA. Interleukin-1β, interleukin-18, and the interleukin-1β converting enzyme. *Ann N Y Acad Sci* 1998; **856**: 1–11.
5 Tassi S, Carta S, Vene R, Delfino L, Ciriolo MR, Rubartelli A. Pathogen-induced interleukin-1β processing and secretion is regulated by a biphasic redox response. *J Immunol* 2009; **183**: 1456–1462.
6 Martinon F, Mayor A, Tschopp J. The inflammasomes: guardians of the body. *Annu Rev Immunol* 2009; **27**: 229–265.
7 Netea MG, Nold-Petry CA, Nold MF, Joosten LA, Opitz B, van der Meer JH *et al.* Differential requirement for the activation of the inflammasome for processing and release of IL-1β in monocytes and macrophages. *Blood* 2009; **113**: 2324–2335.
8 Latz E, Xiao TS, Stutz A. Activation and regulation of the inflammasomes. *Nat Rev Immunol* 2013; **13**: 397–411.
9 Gottipati S, Rao NL, Fung-Leung WP. IRAK1: a critical signaling mediator of innate immunity. *Cell Signal* 2008; **20**: 269–276.
10 Song KW, Talamas FX, Suttmann RT, Olson PS, Barnett JW, Lee SW *et al.* The kinase activities of interleukin-1 receptor associated kinase (IRAK)-1 and 4 are redundant in the control of inflammatory cytokine expression in human cells. *Mol Immunol* 2009; **46**: 1458–1466.
11 Cushing L, Stochaj W, Siegel M, Czerwinski R, Dower K, Wright Q *et al.* Interleukin 1/Toll-like receptor-induced autophosphorylation activates interleukin 1 receptor-associated kinase 4 and controls cytokine induction in a cell type-specific manner. *J Biol Chem* 2014; **289**: 10865–10875.
12 Tiwari RL, Singh V, Singh A, Barthwal MK. IL-1R-associated kinase-1 mediates protein kinase Cδ-induced IL-1β production in monocytes. *J Immunol* 2011; **187**: 2632–2645.
13 Moynagh PN. The Pellino family: IRAK E3 ligases with emerging roles in innate immune signalling. *Trends Immunol* 2009; **30**: 33–42.
14 Daub K, Langer H, Seizer P, Stellos K, May AE, Goyal P *et al.* Platelets induce differentiation of human CD34+ progenitor cells into foam cells and endothelial cells. *FASEB J* 2006; **20**: 2559–2561.
15 Liu W, Yin Y, Zhou Z, He M, Dai Y. OxLDL-induced IL-1β secretion promoting foam cells formation was mainly via CD36 mediated ROS production leading to NLRP3 inflammasome activation. *Inflamm Res* 2014; **63**: 33–43.
16 Hayashi T, Juliet PA, Miyazaki A, Ignarro LJ, Iguchi A. High glucose downregulates the number of caveolae in monocytes through oxidative stress from NADPH oxidase: implications for atherosclerosis. *Biochim Biophys Acta* 2007; **1772**: 364–372.
17 Kim JH, Na HJ, Kim CK, Kim JY, Ha KS, Lee H *et al.* The non-provitamin A carotenoid, lutein, inhibits NF-kappaB-dependent gene expression through redox-based regulation of the phosphatidylinositol 3-kinase/PTEN/Akt and NF-kappaB-inducing kinase pathways: role of H(2)O(2) in NF-kappaB activation. *Free Radic Biol Med* 2008; **45**: 885–896.
18 Bae YS, Lee JH, Choi SH, Kim S, Almazan F, Witztum JL *et al.* Macrophages generate reactive oxygen species in response to minimally oxidized low-density lipoprotein: toll-like receptor 4- and spleen tyrosine kinase-dependent activation of NADPH oxidase 2. *Circ Res* 2009; **104**: 210–218, 21p following 8.
19 Zhang X, Shan P, Jiang G, Cohn L, Lee PJ. Toll-like receptor 4 deficiency causes pulmonary emphysema. *J Clin Invest* 2006; **116**: 3050–3059.
20 Repnik U, Knezevic M, Jeras M. Simple and cost-effective isolation of monocytes from buffy coats. *J Immunol Methods* 2003; **278**: 283–292.
21 Mehta VB, Hart J, Wewers MD. ATP-stimulated release of interleukin (IL)-1β and IL-18 requires priming by lipopolysaccharide and is independent of caspase-1 cleavage. *J Biol Chem* 2001; **276**: 3820–3826.
22 Li Z, Younger K, Gartenhaus R, Joseph AM, Hu F, Baer MR *et al.* Inhibition of IRAK1/4 sensitizes T cell acute lymphoblastic leukemia to chemotherapies. *J Clin Invest* 2015; **125**: 1081–1097.
23 Barthwal MK, Sathyanarayana P, Kundu CN, Rana B, Pradeep A, Sharma C *et al.* Negative regulation of mixed lineage kinase 3 by protein kinase B/AKT leads to cell survival. *J Biol Chem* 2003; **278**: 3897–3902.
24 Grube E, Buellesfeld L. Rapamycin analogs for stent-based local drug delivery. Everolimus- and tacrolimus-eluting stents. *Herz* 2004; **29**: 162–166.
25 Berthier A, Lemaire-Ewing S, Prunet C, Monier S, Athias A, Bessede G *et al.* Involvement of a calcium-dependent dephosphorylation of BAD associated with the localization of Trpc-1 within lipid rafts in 7-ketocholesterol-induced THP-1 cell apoptosis. *Cell Death Differ* 2004; **11**: 897–905.
26 Kumar S, Barthwal MK, Dikshit M. Cdk2 nitrosylation and loss of mitochondrial potential mediate NO-dependent biphasic effect on HL-60 cell cycle. *Free Radic Biol Med* 2010; **48**: 851–861.
27 Singh V, Jain M, Prakash P, Misra A, Khanna V, Tiwari RL *et al.* A time course study on prothrombotic parameters and their modulation by anti-platelet drugs in hyperlipidemic hamsters. *J Physiol Biochem* 2011; **67**: 205–216.
28 Garcia-Calvo M, Peterson EP, Leiting B, Ruel R, Nicholson DW, Thornberry NA. Inhibition of human caspases by peptide-based and macromolecular inhibitors. *J Biol Chem* 1998; **273**: 32608–32613.
29 Shanmugam N, Reddy MA, Guha M, Natarajan R. High glucose-induced expression of proinflammatory cytokine and chemokine genes in monocytic cells. *Diabetes* 2003; **52**: 1256–1264.
30 Forsberg M, Druid P, Zheng L, Stendahl O, Sarndahl E. Activation of Rac2 and Cdc42 on Fc and complement receptor ligation in human neutrophils. *J Leukoc Biol* 2003; **74**: 611–619.
31 Kyriakis JM, Avruch J. Mammalian mitogen-activated protein kinase signal transduction pathways activated by stress and inflammation. *Physiol Rev* 2001; **81**: 807–869.
32 Bedard K, Krause KH. The NOX family of ROS-generating NADPH oxidases: physiology and pathophysiology. *Physiol Rev* 2007; **87**: 245–313.
33 Padgett LE, Burg AR, Lei W, Tse HM. Loss of NADPH oxidase-derived superoxide skews macrophage phenotypes to delay type 1 diabetes. *Diabetes* 2014; **64**: 937–946.
34 Toshchakov V, Jones BW, Perera PY, Thomas K, Cody MJ, Zhang S *et al.* TLR4, but not TLR2, mediates IFN-β-induced STAT1alpha/beta-dependent gene expression in macrophages. *Nat Immunol* 2002; **3**: 392–398.
35 Barrenschee M, Lex D, Uhlig S. Effects of the TLR2 agonists MALP-2 and Pam3Cys in isolated mouse lungs. *PLoS One* 2010; **5**: e13889.

36 Sabroe I, Prince LR, Jones EC, Horsburgh MJ, Foster SJ, Vogel SN *et al.* Selective roles for Toll-like receptor (TLR)2 and TLR4 in the regulation of neutrophil activation and life span. *J Immunol* 2003; **170**: 5268–5275.
37 Yang CS, Shin DM, Kim KH, Lee ZW, Lee CH, Park SG *et al.* NADPH oxidase 2 interaction with TLR2 is required for efficient innate immune responses to mycobacteria via cathelicidin expression. *J Immunol* 2009; **182**: 3696–3705.
38 Wang J, Ouyang Y, Guner Y, Ford HR, Grishin AV. Ubiquitin-editing enzyme A20 promotes tolerance to lipopolysaccharide in enterocytes. *J Immunol* 2009; **183**: 1384–1392.
39 Yang CS, Shin DM, Lee HM, Son JW, Lee SJ, Akira S *et al.* ASK1-p38 MAPK-p47phox activation is essential for inflammatory responses during tuberculosis via TLR2-ROS signalling. *Cell Microbiol* 2008; **10**: 741–754.
40 Mendez-Samperio P, Perez A, Alba L. Reactive oxygen species-activated p38/ERK 1/2 MAPK signaling pathway in the *Mycobacterium bovis* bacillus Calmette Guerin (BCG)-induced CCL2 secretion in human monocytic cell line THP-1. *Arch Med Res* 2010; **41**: 579–585.
41 Dewas C, Fay M, Gougerot-Pocidalo MA, El-Benna J. The mitogen-activated protein kinase extracellular signal-regulated kinase 1/2 pathway is involved in formyl-methionyl-leucyl-phenylalanine-induced p47phox phosphorylation in human neutrophils. *J Immunol* 2000; **165**: 5238–5244.
42 Carta S, Tassi S, Pettinati I, Delfino L, Dinarello CA, Rubartelli A. The rate of interleukin-1β secretion in different myeloid cells varies with the extent of redox response to Toll-like receptor triggering. *J Biol Chem* 2011; **286**: 27069–27080.
43 MacGillivray MK, Cruz TF, McCulloch CA. The recruitment of the interleukin-1 (IL-1) receptor-associated kinase (IRAK) into focal adhesion complexes is required for IL-1β-induced ERK activation. *J Biol Chem* 2000; **275**: 23509–23515.
44 Gaestel M, Kotlyarov A, Kracht M. Targeting innate immunity protein kinase signalling in inflammation. *Nat Rev Drug Discov* 2009; **8**: 480–499.
45 Kogut MH, Genovese KJ, He H. Flagellin and lipopolysaccharide stimulate the MEK-ERK signaling pathway in chicken heterophils through differential activation of the small GTPases, Ras and Rap1. *Mol Immunol* 2007; **44**: 1729–1736.
46 Koziczak-Holbro M, Gluck A, Tschopp C, Mathison JC, Gram H. IRAK-4 kinase activity-dependent and -independent regulation of lipopolysaccharide-inducible genes. *Eur J Immunol* 2008; **38**: 788–796.
47 Kollewe C, Mackensen AC, Neumann D, Knop J, Cao P, Li S *et al.* Sequential autophosphorylation steps in the interleukin-1 receptor-associated kinase-1 regulate its availability as an adapter in interleukin-1 signaling. *J Biol Chem* 2004; **279**: 5227–5236.
48 Pauls E, Nanda SK, Smith H, Toth R, Arthur JS, Cohen P. Two phases of inflammatory mediator production defined by the study of IRAK2 and IRAK1 knock-in mice. *J Immunol* 2013; **191**: 2717–2730.
49 Li S, Strelow A, Fontana EJ, Wesche H. IRAK-4: a novel member of the IRAK family with the properties of an IRAK-kinase. *Proc Natl Acad Sci USA* 2002; **99**: 5567–5572.
50 Pedram A, Razandi M, Levin ER. Extracellular signal-regulated protein kinase/Jun kinase cross-talk underlies vascular endothelial cell growth factor-induced endothelial cell proliferation. *J Biol Chem* 1998; **273**: 26722–26728.
51 Zhang W, Liu HT. MAPK signal pathways in the regulation of cell proliferation in mammalian cells. *Cell Res* 2002; **12**: 9–18.
52 Jeon YJ, Han SH, Lee YW, Lee M, Yang KH, Kim HM. Dexamethasone inhibits IL-1β gene expression in LPS-stimulated RAW 264.7 cells by blocking NF-kappa B/Rel and AP-1 activation. *Immunopharmacology* 2000; **48**: 173–183.
53 Cruz CM, Rinna A, Forman HJ, Ventura AL, Persechini PM, Ojcius DM. ATP activates a reactive oxygen species-dependent oxidative stress response and secretion of proinflammatory cytokines in macrophages. *J Biol Chem* 2007; **282**: 2871–2879.
54 Fernandes-Alnemri T, Kang S, Anderson C, Sagara J, Fitzgerald KA, Alnemri ES. Cutting edge: TLR signaling licenses IRAK1 for rapid activation of the NLRP3 inflammasome. *J Immunol* 2013; **191**: 3995–3999.
55 Lin KM, Hu W, Troutman TD, Jennings M, Brewer T, Li X *et al.* IRAK-1 bypasses priming and directly links TLRs to rapid NLRP3 inflammasome activation. *Proc Natl Acad Sci USA* 2014; **111**: 775–780.
56 Cathcart MK. Regulation of superoxide anion production by NADPH oxidase in monocytes/macrophages: contributions to atherosclerosis. *Arterioscler Thromb Vasc Biol* 2004; **24**: 23–28.
57 Obenauer JC, Cantley LC, Yaffe MB. Scansite 2.0: Proteome-wide prediction of cell signaling interactions using short sequence motifs. *Nucleic Acids Res* 2003; **31**: 3635–3641.
58 Kampfrath T, Maiseyeu A, Ying Z, Shah Z, Deiuliis JA, Xu X *et al.* Chronic fine particulate matter exposure induces systemic vascular dysfunction via NADPH oxidase and TLR4 pathways. *Circ Res* 2011; **108**: 716–726.